Microelectronic Engineering 199 (2018) 1–15

Contents lists available at ScienceDirect

Microelectronic Engineering

journal homepage: www.elsevier.com/locate/mee

Research paper

Microfluidic approaches for the design of functional materials

Kyoung-Ku Kang, Byungjin Lee, Chang-Soo Lee*

Department of Chemical Engineering and Applied Chemistry, Chungnam National University, 99 Daehak-ro, Yuseong-gu, Daejeon 34134, Republic of Korea

ARTICLE INFO

Keywords:
Microfluidics
Droplet-based microfluidics
Microparticles
Polymeric microparticles
Inorganic particles
Janus particles

ABSTRACT

Microfluidic systems, including microreactors, can precisely control an entire process and provide advantages, such as rapid mixing, fast heat and mass transfer due to miniaturization. Above all, the advantage of being easy to design and fabricate is the most attractive for the purposes of researchers. In the past two decades, it has become a research topic of great interest in the field of synthesis of chemicals and materials, due to these unique advantages. Furthermore, in recent years, studies are actively underway to design, construct, and compose the elements and functions of microfluidic devices for designing and synthesizing materials for specific applications or purposes. In this review, we will discuss the principles and forms of basic microfluidic devices, and discuss how microfluidic devices are used in the synthesis of polymeric and inorganic materials, particularly functional materials. Finally, we will present how microfluidic systems will be used in future materials research.

1. Introduction

Over the last decades, the area of particulate materials synthesis has evolved rapidly due to the development of analysis and synthesis technologies. The development of synthesis methods and processes has also contributed greatly to the development of materials research. Droplet-based microfluidics has become one of the most widely used tools in material synthesis, because of their advantages, which include producing monodisperse droplets, consuming small reagents, facilitating rapid reactions due to their high surface area-to-volume ratio, and their independent control characteristics. Polymeric and inorganic materials prepared by microfluidics have been reported to be the most synthesized and applied functional materials. In particular, in the case of polymer materials, the synthesis of micrometer-sized particles with various functionalities and morphologies is the most studied, and in the case of inorganic materials, nanoparticles with various sizes and crystal structures are the most studied. Furthermore, these polymers and inorganic materials as functional materials have also been widely applied to the fields of medicine, biology, chemistry, physics, electricity, electronics, nanotechnology, biotechnology, and clean and reusable energy, synthesis of photonic materials, micro-objects, consumer and personal care products, particle-based display technologies, field-responsive rheological fluids, therapeutics, tissue engineering scaffolds, high-performance composite filler materials, and food additives [1–14].

In general, the functions of polymers and inorganic materials are strongly affected by their physicochemical properties, such as compositions, surface nature, morphology, particle size, and uniformity. Furthermore, these are also important determinants of application possibilities and achievements [15]. Therefore, it is desirable to use uniform and homogeneous droplets, which are precisely controlled, to ensure stable, controlled and predictable results in application fields. Therefore, a deep and systematic understanding of the synthesis method and process is necessary. In particular, it will be more necessary when designing and manufacturing new functional materials. However, most polymeric and inorganic nanoparticles are typically synthesized using traditional chemical reactors, and the reaction conditions of these chemical reactors are difficult to uniformly control, such as mixing, temperature control and flow control. These difficulties can affect the properties, such as the molecular weight, morphology, size and crystallinity of the synthesized materials, which also influence the functionality of these materials. Therefore, various synthetic processes and methods have been developed to overcome the difficulties of these conventional synthesis methods [16–23]. Droplet-based microfluidics, in comparison with chemical reactors, offer excellent control of a wide range of overall reaction conditions, such as fast mixing, short residence times, precise reaction temperature control and well-defined rheological flow [24,25]. These high reaction control capabilities are the result of high heat and mass transfer rates based on small droplet size and flow. Even, droplet-based microfluidics can be combined with real-time analysis and feedback control to instantly adjust the synthesis conditions. This is the greatest advantage in designing and synthesizing functional particles using droplet-based microfluidic devices, and these advantages can present a new paradigm in material synthesis. Furthermore, because of these unique advantages, droplets formed through

* Corresponding author.
E-mail address: rhadum@cnu.ac.kr (C.-S. Lee).

https://doi.org/10.1016/j.mee.2018.07.007
Received 28 December 2017; Received in revised form 15 June 2018; Accepted 19 July 2018
Available online 20 July 2018
0167-9317/

microfluidics can be directly used as a microreactor for chemical and biochemical reactions.

The purpose of this article is to review recent advances in particulate materials, i.e., polymeric and inorganic particles, that take advantage of droplet-based microfluidics. First, the principle of the droplet-based microfluidic reactor will be briefly introduced. Next, the representative synthesis method and the results of polymer microparticles and inorganic particles will be explained. In addition, we will introduce each advantage, application and possibility of the synthesized functional material. Finally, it provides a perspective on future microfluidic device developments.

2. Considerations for design of microfluidics

2.1. Dimensionless number in designing of microfluidics

To obtain well-defined droplets, the dripping and jetting flow regions must be predicted. By predicting the flow pattern of the fluid flowing through the microfluidic channel, it is possible to generate and stabilize droplets in the microfluidic device. Therefore, this is important in determining the success of the synthesis of the functional materials using droplets generated in microfluidics. Predicting the flow patterns is possible using the geometry of the designed channel, the physical properties of the fluid and the several dimensionless numbers calculated by combining these properties. This series of efforts is the first step in the design of functional materials and droplet-based microfluidics. Prediction of flow patterns is possible using the physical properties of the fluid flowing through the microfluidic channel and the dimensionless number calculated by combining these properties.

Droplet-based microfluidics can be generated with the specific flow patterns of microfluidics, such as a dripping, at a part of the jetting region, as shown in Fig. 1. The dripping and jetting region in each microfluidic device can be controlled by several fluidic physical parameters, such as the geometries of the devices, ratio of the flow rates of the multiple fluids, densities of fluids (ρ), interfacial tension (γ) and viscosities of the fluids (μ). There are several dimensionless numbers that can be determined by the physical parameters of the fluids [26–28]. Among the many dimensionless numbers, we briefly introduce representative numbers in microfluidics that are very useful for predicting and controlling the flow from the dripping to the jetting regime in microfluidics.

2.2. Reynold number (Re)

The Reynolds number (*Re*) is an important dimensionless number affecting the flow pattern of the fluid for the formation of stable droplets in the microfluidic system. *Re* is expressed as the ratio between inertial force and viscous force and is widely used to predict fluid flow behavior. This *Re* can be calculated from the correlation between the physical properties of the fluid and the geometry of the microfluidic and predict the flow pattern of the fluid, where U is the characteristic velocity of fluid and D_H is the hydraulic diameter of microchannel. D_H is defined as $4A/P$, where A is the cross-section through which the fluid flows and P is the wetted perimeter of the cross-section. D_H is widely used to handle flows in various types of channels, both circular and non-circular. Generally, the *Re* is in the range of 10^{-6} to 10 for microfluidics [27]. For most droplet-based microfluidics, the *Re* is < 1 because the channel size is in the micrometer-scale. Therefore, the viscous force is dominant over the fluid inertia and has laminar flow, in the case of a microfluidic system with such low *Re*.

$$Re = \frac{\rho U D_H}{\mu}$$

2.3. Capillary number (Ca)

The generation of droplets is caused by the sequential change of the interface between the dispersed phase and continuous phase [29]. The change of interface is caused by the interfacial tension between two fluids flowing through the channel of microfluidics, and the interfacial tension plays a key role in droplet generation [30–35]. These considerations promote the investigation of several dimensionless numbers [27]. One of these, the capillary number (*Ca*) is the most commonly used dimensionless number, which is the ratio of viscous force to capillary force. The *Ca* is defined by using the interfacial tension and viscosity and is presented by the viscosity of the fluid (μ), characteristic velocity (U) and interfacial tension (γ). Usually, the inertial force does not directly depend on the length of the device. However, when the device length is reduced, viscous stress and capillary pressure increase, whereas the gravitational force is decreased.

Therefore, the *Ca* of microfluidic devices generally ranges between 10^{-3} and 10, and is also affected by viscosity and capillary force [36–38]. This physical meaning also indicates that the *Ca* is the most

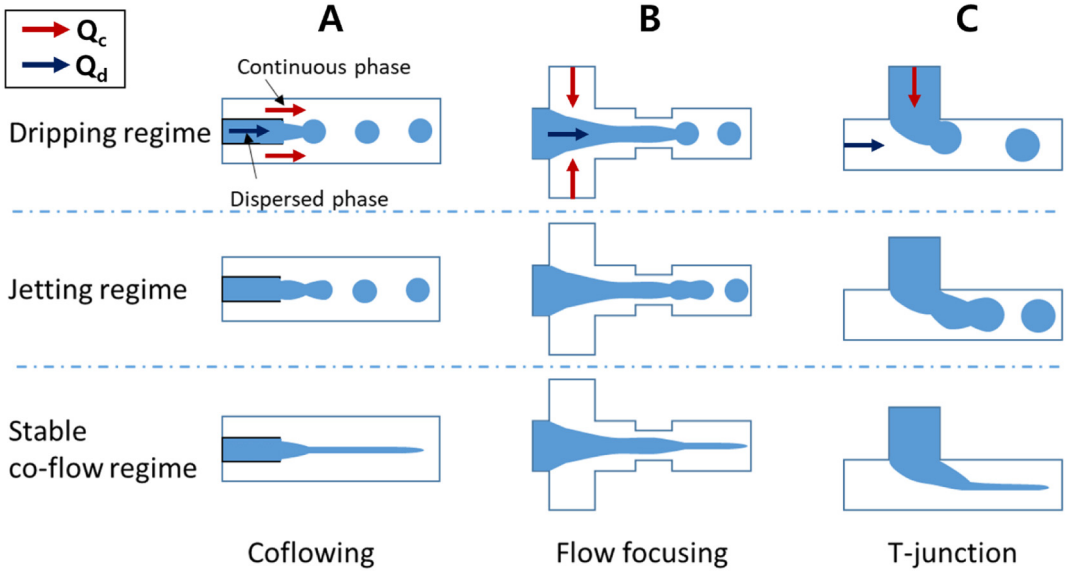

Fig. 1. Representative microfluidics and their flow patterns. (A) T-junction microfluidic device, (B) flow-concentrated microfluidic device, and (C) microfluidic device. Q_d and Q_c represent the flow rate of the disperse phase and the continuous phase, respectively.

widely used dimensionless number in microfluidic droplet generation [34,39–44].

$$Ca = \frac{\mu U}{\gamma}$$

2.4. Weber number (We)

Fluid inertia is negligible for most microfluidic flows. However, in case of coflowing with a high flow velocity, jetting and other flow pattern increase. In this case, the inertial and capillary forces have dominant roles compared to the viscous stresses, and the Webber number can become an important dimensionless number [26,45]. The Weber number (*We*) is the product of *Re* and *Ca*, and defined as the ratio between the inertial force and the surface tension force, where *d* is the characteristic diameter of the fluid. The *We* is also considered to be a significant number when the inertial and capillary forces have dominant roles compared to the viscous stresses, such as the formation of jetting during coflowing with a high flow rate. The *We* is < 1 for most microfluidics.

$$We = Re{\cdot}Ca = \frac{\rho d U^2}{\gamma}$$

3. Representative geometry of droplet-based microfluidics

The most widely used channel types for liquid-based microfluidic systems are T-junctions, flow-focusing and coflowing, as shown in Fig. 1. During the generation of the droplets, these devices are commonly operated by using two different phase fluids. The formation of well-defined droplet is similar to the emulsion system of oil and water [46–52]. Depending on the nature of the channel surface, the dispersed phase is commonly an aqueous phase containing a small amount of emulsifier and the continuous phase is an oil-like phase as a counterpart. The emulsifier in the dispersed phase improves the stability of the droplets.

Previously, the mechanism of formation of droplet has been investigated experimentally and theoretically. The dynamic process of the droplet formation is able to provide useful information for the understanding of the different flow pattern regime [26,28,29,53–57]. In 2013, Nune et al. summarized and reported the formation of the dripping, transition, jetting, co-flow and their mechanisms by numerous simulations and experiments [45]. The well-defined spherical droplets are generated under the specific flow patterns that are formed within the channels of a microfluidic device. In addition, these flow patterns are dominated by the flow rate and the physical properties of the fluids. The most representative flow patterns are dripping, jetting and co-flow, which represent unique flow profiles. The spherical droplets dealt with in this article are mainly generated by the dripping flow pattern, but some of them are generated in the jetting flow pattern, depending on the design and structure of microfluidic devices.

3.1. T-junction microfluidics

The schematic illustration of the operating condition of the T-junction is shown in Fig. 1A. The dispersed phase is fed to the side channel, and the continuous phase is injected into the main channel. The T-junction device was first reported by Thorsen et al. to produce monodisperse water droplet in oil as a continuous phase [58]. Since this report, T-junction and similar forms of microfluidics have been widely used due to their simplicity and ability to produce monodisperse droplets. Studies on the geometric changes of T-junctions have continued and have been reported recently [31,32,44,59–65]. In fact, with the basic T-junction structure, achieving the requirements for various application fields is difficult. Therefore, geometric changes to T-junctions have recently been studied and reported. Changes to the junction angle of the channel in the T-junction have been studied, and they affect the generation phenomena of the droplet and the resultant droplets [54,66–68]. Materials for more complex applications are produced through the creation and merging of two different droplets, which requires the manufacture of two or more droplets in one reactor. Various types of multiple junctions have been proposed to meet this need. The various modified T-junctions, such as the K-junction and V-junction, have been developed to control the size, composition, and generating frequency, required for biochemical analysis [66,69–71]. In addition, for several special application, T-junction microfluidics have recently been applied in designing microvalves and microactuators, as well [72,73].

When droplets are generated by using this T-junction microfluidics, three distinguishable flow regimes, squeezing, dripping, and jetting, can be observed, depending on the physical parameters of the fluids. The emergence of each flow pattern is closely related to the capillary number (*Ca*) and the difference of flow rate between the two fluids flowing through the channel. At low *Ca* ($< 10^{-2}$) values, the shear forces are not sufficient to distort the disperse phase, resulting in confined fluidic environments formed by blocking the channel through the growth of the disperse phase. In this state, the disperse phase increase its resistance, while a thin film of the continuous phase between the disperse phase and the wall of the device is generated at the T-junction. This squeezes the disperse phase, eventually breaking up the disperse phase into droplets. This type of pressure-dominated formation of droplets is known as “squeezing”.

Above a relatively higher *Ca* ($10^{-2} < Ca < 10^{-1}$) value, the continuous phase strongly affects the dispersed phase at the junction, causing breakup into droplets. This shear-driven formation of droplets is referred to as “dripping”. In this regime, the sizes of the droplets can be controlled by the *Ca* and the ratio of the flow rates between the continuous phase (Q_c) and disperse phase (Q_d) [44,74]. For example, Garstecki et al. demonstrated that the droplet size formed at low *Ca* values mainly depends on the flow rate ratio of the disperse phase and the continuous phase (Q_d/Q_c) [44]. The size of droplets formed at low *Ca* is larger than the width of the microchannel. At even higher *Ca* ($> 10^{-1}$) values, jetting or coflowing occurs [35,40,75]. For example, Gupta et al. demonstrated that jetting and stable coflowing were generated as the *Ca* increased from 0.1 to 0.3 within the given dimensions of the T-junction microfluidic devices [40]. In addition, Guillot and Colin showed that stable coflowing developed as the flow rate of the disperse phase overcame that of the continuous phase, and the critical values of the flow rate were decreased by increasing the viscosity of the disperse phase [75,76].

3.2. Flow-focusing microfluidics

The flow-focusing approach was first introduced by Anna et al., [77]. It is also one of the most general methods to study the fluidic evolution from the dripping to jetting regime by manipulating the physical parameters of the fluids [37,54,78–87]. In this method, two immiscible fluids comprise a continuous phase and a disperse phase and they are introduced into each inlet. The two fluids are flow-focused into a small orifice, as shown in Fig. 1B. In this fluidic state, the continuous phase causes a symmetrical shear force that affects the disperse phase, resulting in an elongated fluidic state. The elongation-dominated velocity field of the continuous phase consistently stretches the disperse phase into a thin jet, finally breaking up the thread into droplets. For example, Liu and Zhang reported that the dripping-to-jetting transition is controlled by increasing the ratio of the flow rates (Q_d/Q_c) from 0.6 to 3 at a given *Ca* (0.004). Humphry et al. revealed that the boundary condition between stable and unstable coflowing occurred at $Q_d/Q_c \fallingdotseq 0.58$. In addition, the size of the droplets was controlled by simply varying the *Ca* and the ratio of the flow rates [54,88,89].

3.3. Co-flowing microfluidics

The co-flowing method is a simple approach to form droplets, which was first utilized by Umbanhowar et al. at the macroscale, and several

other researchers have also brought it to the microscale [53,55,56,90–96]. Coflowing microfluidic devices are generally comprised of a set of concentric capillaries, inner and outer capillaries in a coaxial direction. The continuous phase and dispersed phase are individually injected through each capillary, forming a parallel flow, as shown in Fig. 1A. The Plateau-Rayleigh instability explains the phenomenon where a falling jet or cylinder of fluid at one point ceases to be a jet and breaks into multiple droplets of smaller total surface area. In the microfluidics with two immiscible fluids [33,97–99], the disperse phase becomes unstable due to interfacial tension, minimizing the interfacial area, which is known as Rayleigh-Plateau instability. This principle accounts for the formation of droplets due to thread breaks in the flow stream of fluid. For example, Utada et al. demonstrated that when each flow rate is low, droplets are formed at the tip of the inner capillary, which is known as dripping. When the ratio of the flow rates (Q_c/Q_d) is increased, the size of the droplets decreases. When the size of the droplets is approximately that of the tips, the fluids enter the jetting regime, which eventually becomes unstable due to the Rayleigh-Plateau instability. This result eventually leads to the formation of droplets at the tip of the extended jet. In this state, increasing the fluid velocity is favorable, enabling the formation of stable jetting. In contrast, absolute stability [100–104] is dominant at low *Ca* values, leading to disturbances in the fluid velocity. These results allowed the fluids to break into droplets [105]. The capillary number (*Ca*) and ratio of the flow rates are major parameters for controlling the dripping regime and the jetting regime.

4. Microfluidic approaches for functional materials from emulsion droplets

In this section, we review several studies to generate multifunctional microparticles from emulsion droplets. We divided this section into two categories: (1) the poly(dimethylsiloxane) device (PDMS device), (2) and the glass capillary device, based on the materials used for the microfluidic device. PDMS is a material that has been widely used for microfluidic devices since it has the unique features of good processability, high transparency, and flexibility. Despite the distinctive properties of PDMS, it has limitations as a microreactor because of its intrinsic high hydrophobicity, poor chemical compatibility and solvent resistance, which is often a requirement in chemical reactions. As an alternative, microfluidic devices fabricated with glass capillaries have attracted much attention due to its good chemical and solvent compatibility. Moreover, the glass capillary device does not require the photolithography process for the master mold, or multiple junctions for complex emulsions. It also has round cross-section profiles, while PDMS is mainly rectangular, which can be a significant parameter for shaping particles. The comparative advantage and disadvantage of PDMS and glass capillary-based microfluidic devices are summarized in Table 1.

The type of emulsification is another important factor for functional microparticles, with consideration of the thermodynamics between liquid phases constituting emulsions. There are two main approaches to generating complex emulsions: 1) thermodynamically stable emulsion formation and 2) induced phase separation. Thermodynamically controlled liquid phases form a stable emulsion based on a spreading coefficient, a thermodynamic parameter that determines the wettability of the surface to a given liquid [114]. It is possible to generate double emulsions such as W/O/W, O/W/O, and more complex emulsion, such as triple emulsions and quadruple emulsions. However, it is a relatively difficult to precisely control the composition of each phase since it relies on the hydrodynamic parameters, such as flow rate, viscosity, and interfacial tension. An alternative method is to induce phase separation of a single phase of a mixture. The basic principles of phase separation are based on the shift of equilibrium by additives to a temporarily stable single-phase of the mixture. The phase separation occurs via spinodal decomposition or nucleation and growth [115–117]. Spinodal decomposition is a mechanism by which a solution of two or more components decomposes into equilibrium coexisting phases with different chemical compositions and physical properties [115,116]. This phenomenon is derived by a shift of relative miscibility of each component in the system [117]. In case of nucleation and growth, nuclei are initially formed in nucleation zone in a supersaturated solution and grow until reach a boundary, which is presented between metastable and undersaturated zone of the solubility curve [117]. It is possible not only to control the composition of each compartment by tuning the composition of the mixture but also to fabricate highly porous materials that exploit the spinodal decomposition with a controlled reaction time. It is important to select a proper type of device with consideration for the type of material, solvent, physical and chemical properties of the material, and the profile that sometimes limits the shape of generated particles. In the following subsections, we introduce several examples of multifunctional microparticles based on the two strategies (Table 2).

4.1. Poly(dimethylsiloxane) based microfluidic approaches

Since PDMS, with its various advantages, was first introduced into microfluidics by George Whitesides, many researchers have focused on its application to functional materials [106]. PDMS-based approaches have also been used to design efficient carriers for the encapsulation of drugs, peptides, proteins and cells that can be utilized in various biomedical applications [127–129]. In particular, biopolymer-based hydrogels have been demonstrated as suitable materials due to their biocompatibility, low toxicity, and biodegradability.

Geest et al. found that biodegradable monodisperse hydrogels composed of dextran hydroxyethyl methacrylate (dex-HEMA) can be conveniently produced using microfluidic devices [118]. A W/O emulsion (dex-HEMA in oil) was formed in the microchannels, and then, UV irradiation was used to form monodisperse dex-HEMA hydrogels (9.9 μm ± 0.3 μm), as shown in Fig. 2A. The hydrogels showed an excellent property that releases pre-entrapped proteins (FITC-BSA) within 30 s due to the spontaneous degradation of dex-HEMA. This mechanism was triggered by hydrolysis in a sodium hydroxide solution, as shown in Fig. 2B. Encapsulation of bioactive materials in alginate

Table 1
Representative advantages and disadvantages of PDMS-based and glass capillary-based devices.

Types of device	Advantages	Disadvantages	Ref.
PDMS-based device	• Reproducible fabrication • Compatible for oil continuous phase due to hydrophobic surface • Flexibility for on-chip microvalve fabrication	• High fabrication cost • Poor solvent resistance • Surface modification required for use of hydrophilic solution • Short persistency of surface modification	[106–110]
Glass capillary-based device	• Cost-effective • Compatible for water continuous phase due to hydrophilic surface • Good solvent resistance • Semi-permanent surface modification	• Low reproducible fabrication • Impossible to fabricate on-chip microvalves • Surface modification required for use of hydrophobic solution	[111–113]

Table 2
Examples of functional microparticles via microfluidic approaches.

Preparation of templates	Features	Materials	Solvent	Appearance	Ref.
PDMS, Flow focusing	Biodegradable hydrogels	dex-HEMA	Mineral oil	Spherical	[118]
PDMS, Phase separation	One-step generation of multiple emulsion	PEGDA	Hexadecane, DEAP	Multiple emulsion	[119]
Etched glass chip, Flow focusing	Electrically anisotropic Janus microspheres	Isobornyl acrylate	Aqueous solution	Janus sphere	[120]
Capillary device, Coflowing	Superhydrophobic Janus particles	ETPTA, SiO_2, α-Fe_2O_3	Aqueous solution	Spherical	[121]
Capillary device, Phase separation	Selective cargo loading, vesicle formation	DEP	Ethanol, water	Multiple emulsion	[122]
Capillary device, Coflowing	Enhanced cargo retainable capsule	ETPTA	Aqueous solution	Triple emulsion	[123]
Capillary device, Coflowing	Crystalline colloid array with high stability	ETPTA, Polystyrene	Aqueous solution	Double emulsion	[124]
Capillary device, Coflowing	Thermosensitive microgels	Poly(NIPAm)	Silicone oil, aqueous	Spherical	[125]
Capillary device, Coflowing	Polymersomes	PBA-PAA diblock copolymer	THF-toluene, aqueous	Spherical polymersome	[126]

beads is also an important issue [130,131]. Many researchers have developed microfluidic approaches for the production of biomolecules trapped in alginate hydrogels [127,129,132–135]. Specifically, spherical alginate hydrogels were formed by controlling the gelation conditions (time, crosslinking agents), as shown in Fig. 2C [127]. Similarly, Choi et al. demonstrated that the in situ encapsulation of cells in monodisperse alginate hydrogels could be conducted using microfluidic devices [136]. They utilized a microfluidic device with a specific geometry to achieve rapid emulsion formation and high mixing efficiency. An alginate solution and a mixture of a yeast cell suspension and a calcium ion solution were injected into each inlet and met at the T-junction, leading to the shear-force-driven breakup to form the monodisperse emulsion. Subsequently, the droplets are gelled rapidly by chaotic mixing driven by the channel geometry, allowing in situ encapsulation of cells in the monodisperse alginate hydrogels (coefficient value $< 1.1\%$), as shown in Fig. 2D. It is expected that the microfluidic approach for the formation of alginate hydrogels can potentially be used as drug carriers, transplantation, biosensors, microreactors and artificial cells [136].

The shape of the particles plays a pivotal role in many applications, such as in the barcoding system, biomedical field, and drug delivery. One of the critical drawbacks of conventional methods is the difficulty in forming geometrically anisotropic particles (non-spherical particles) due to thermodynamically driven surface minimization of droplets [58,77,137,138]. To overcome the drawbacks, several pioneers have offered novel microfluidic approaches based on the control of the hydrodynamic parameters, such as aspect ratio of the microfluidic channels and the volume of the droplets. These approaches have enabled the formation of non-spherical emulsions within confined microfluidic devices, leading to the formation of geometrically anisotropic particles [139,140]. Dendukur et al. demonstrated the formation of non-spherical particles via the in situ UV irradiation of O/W emulsions formed using a T-junction microfluidic device [140]. The plug-shaped Norland Optical Adhesive (NOA) emulsion (O/W) was formed at low *Ca* values by changing the flow rates of the continuous phase (Q_c), while the disk-shaped NOA emulsion as formed by confining the droplets in shallow

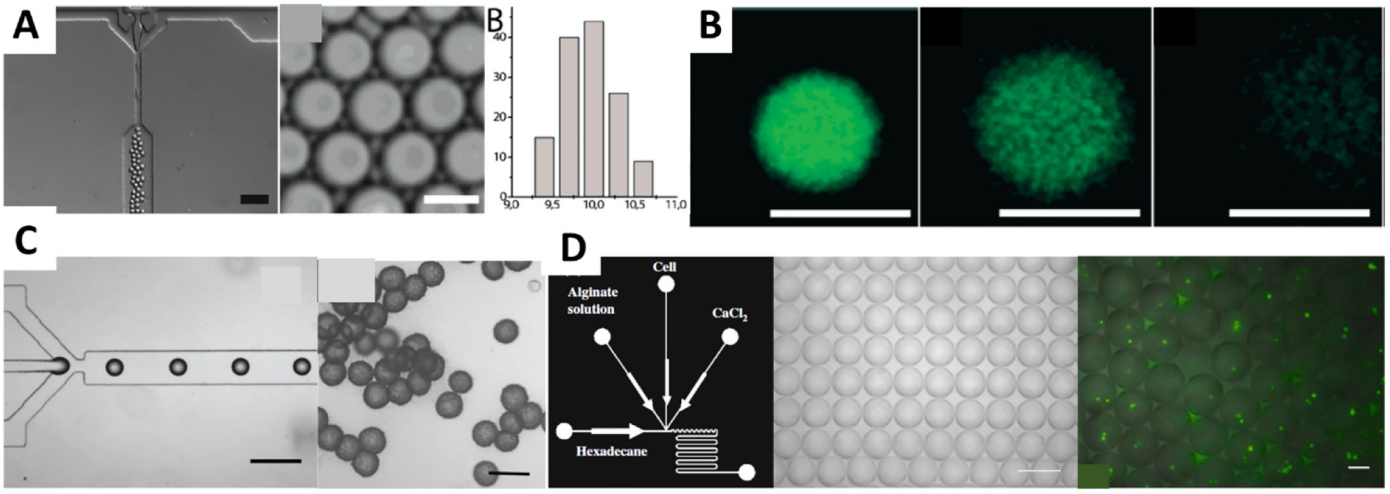

Fig. 2. Formation of functional microspheres via PDMS microfluidic devices and their versatile applications as drug delivery systems, biodegradable hydrogels, and cell encapsulants. (A) Biodegradable dex-HEMA hydrogels (left) and their optical images (middle), indicating their size distribution uniformity (right). (B) Time-lapse images showing the spontaneous release of FITC-BSAs (green) from the dex-HEMA hydrogels by hydrolysis. (C) Spherical alginates in a microfluidic device with controlled gelation conditions (left) and their optical images showing monodisperse alginate microspheres (right). Reproduced with permission from ref. [118] for (A, B) and [127] for (C) Copyright 2005 and 2006 American Chemical Society. (D) A scheme showing the specific geometry for the in situ encapsulation of yeast cells in alginate hydrogels (left), an optical image showing monodisperse alginate hydrogels (middle), and a merged image showing in situ encapsulation of yeast cells (fluorescently tagged with GFP) in the alginate hydrogels. Reproduced with permission from ref. [136]. Copyright 2007 Springer Nature. (For interpretation of the references to color in this figure legend, the reader is referred to the web version of this article.)

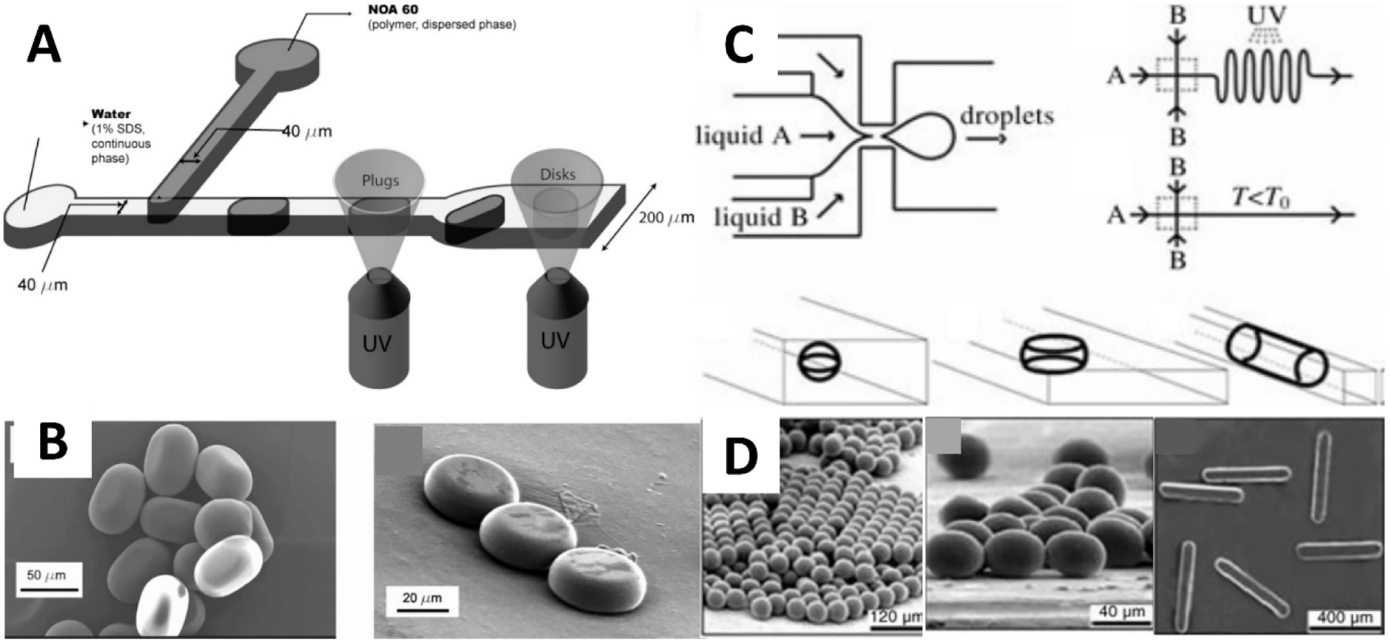

Fig. 3. Formation of non-spherical microparticles with controlled dimensions of the microchannels and volume of droplets. (A) A scheme describing the formation of plug and disk microparticles in T-junction microfluidic device. (B) Scanning electron microscopy (SEM) images of plug and disk-shaped microparticles. Reproduced with permission from ref. [140] Copyright 2005 American Chemical Society. (C) A scheme of flow-focusing geometry used for the formation of (D) microsphere, ellipsoid and rod-shaped microparticles in a flow-focusing microfluidic device. Reproduced with permission from ref. [139]. Copyright 2005 Wiley-VCH.

microchannels. The solidified droplets formed monodisperse plug- and disk-like particles, as shown in Fig. 3A and B. Similarly, Xu et al. showed the formation of spherical and non-spherical particles using UV irradiation on emulsions formed with flow-focusing microfluidic devices [139]. According to their report, the shapes of the particles, such as microspheres, rods, disks, and ellipsoids, were predetermined by the confined microchannels, as shown in Fig. 3C, D. The shapes of the generated emulsion were highly dependent on the height and width of the microchannels.

Geometrically and chemically anisotropic microparticles have been extensively studied due to their unique properties and potentials for various applications [141–149]. Specifically, Janus particles with two discrete properties, such as chemical compositions, geometries, functionalities, electromagnetic properties and other properties, are considered attractive materials for displays, photonic sensors, self-propelled objects, pickering emulsions, and building blocks for self-assembly [120,150–153]. PDMS-based approaches with finely controlled hydrodynamic parameters have become a promising route for generating Janus particles with high uniformity [120,154–158]. Prasad et al. demonstrated the formation of inorganic-organic hybrid Janus microspheres with PDMS-microfluidic device integrated with in situ UV polymerization. Organic and inorganic monomers, composed of functionalized perfluoropolyether (PFPE) and hydrolytic allylhydridopolycarbosilane (AHPCS), were individually introduced into each inlet, and they subsequently meet each other at a junction with a 2% SDS aqueous solution (continuous phase), resulting in a Janus emulsion with two distinctive compartments. The generated Janus emulsions were subsequently exposed to UV radiation, forming hybrid Janus microspheres with distinctive inorganic-organic properties and high uniformity (CV < 3.5%), as shown in Fig. 4A, B [154]. In addition, the size of the organic and inorganic compartments could be modulated by increasing the *Ca* of the organic and inorganic phases, allowing the formation of asymmetric Janus microspheres, as shown in Fig. 4C.

Okushima et al. presented the formation of double emulsions and the controllability of the emulsion size as well as the number of core droplets by double T-junction PDMS-based microfluidic devices [159,160]. The double emulsions were generated by sequential two-step emulsification within the microchannels. An aqueous phase was broken up by the oil phase at the hydrophobic T-junction, followed by the resultant W/O emulsion flowing through the hydrophilic T-junction. At the second junction, the W/O emulsions were additionally emulsified by the aqueous phase, which led to the formation of uniform W/O/W double emulsions, as shown in Fig. 5A. The size of the inner and outer droplets and the number of inner droplets can be tuned with the variation of flow rates, as shown in Fig. 6B. Moreover, they demonstrated selective encapsulation of different inner droplets at the cross junction while two types of droplets are generated alternatively, as shown in Fig. 5C. The capability to design the configuration of inner droplets encapsulated in double emulsions is expected to be a promising tool for droplet-based assays and multiplexed assays [161–163].

Choi et al. recently reported an alternative for generating complex emulsions based on triggered phase separation within a simple microfluidic device [119]. In brief, a dispersed phase composed of a monomer and a good solvent for the monomer, and a continuous phase composed of a separation agent (SA) and a good solvent for the SA, were used to form a single emulsion. In this state, the SAs in the continuous phase diffused into the disperse phase, leading to the phase separation of the single phase of emulsions into complex emulsions, as shown in Fig. 6A and B. The types of emulsions, double, triple, and quadruple emulsions, were controlled by the rate of phase separation, as shown in Fig. 6C. Moreover, the combinatorial modulation of the phase separation and the dewetting processes further transformed the emulsions into Janus double and Janus triple emulsions due to the changing interfacial energy, as shown in Fig. 6D. In addition, they also demonstrated that the selective encapsulation of components could be simultaneously achieved during the emulsification process. Water-soluble fluorescent dyes (red color) were selectively encapsulated into the water-rich phase of the quadruple emulsions based on their relative solubility, as shown in Fig. 6E and F. In contrast, the hydrophobic fluorescent dyes (green color) were present outside the water-rich phase. These results are encouraging for the facile encapsulation of drugs into selective compartments without complicated processes, and for designing anisotropic particles from complex emulsion templates.

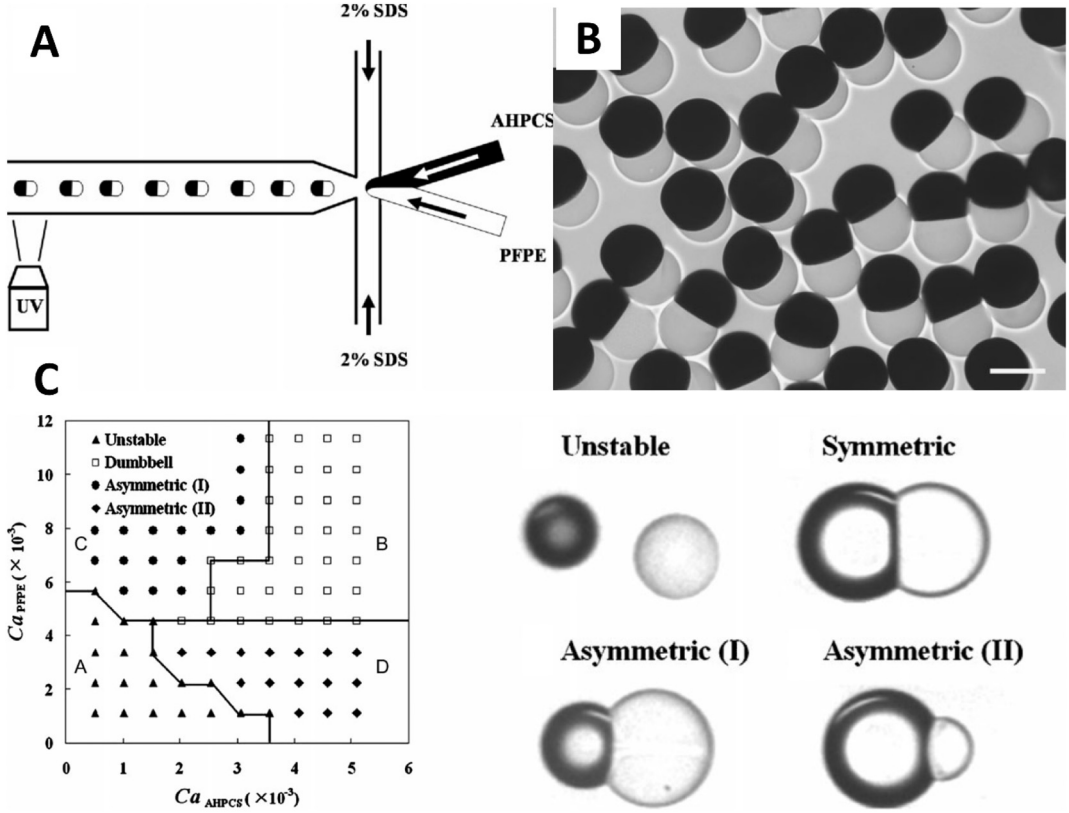

Fig. 4. Generation of Janus hybrid microspheres via controlling *Ca* in a microfluidic device. (A) Janus microspheres with organic (PEPE) and inorganic (AHPCS) substances with flow-focusing microfluidic channels integrated with in situ UV polymerization (B) Optical micrographs showing monodisperse Janus microspheres with PFPE (lighter) and AHPCS compartments (darker). (C) A phase diagram of the Janus microspheres controlled by the *Ca* (left) and four distinctive regimes (right). Reproduced with permission from ref. [154] for (A–C). Copyiright 2009 and 2006 Wiley-VCH.

4.2. Glass capillary microfluidic approaches

In PDMS-based microfluidics, multiple emulsions, as a template for functional microparticles, are typically made in a two-step emulsification process. However, the sequential emulsification process limits the range of the flow rate, and it often yields poorly controlled emulsions in terms of size and configurations. Moreover, its poor chemical compatibility limits the applicable polarity of the solvents and

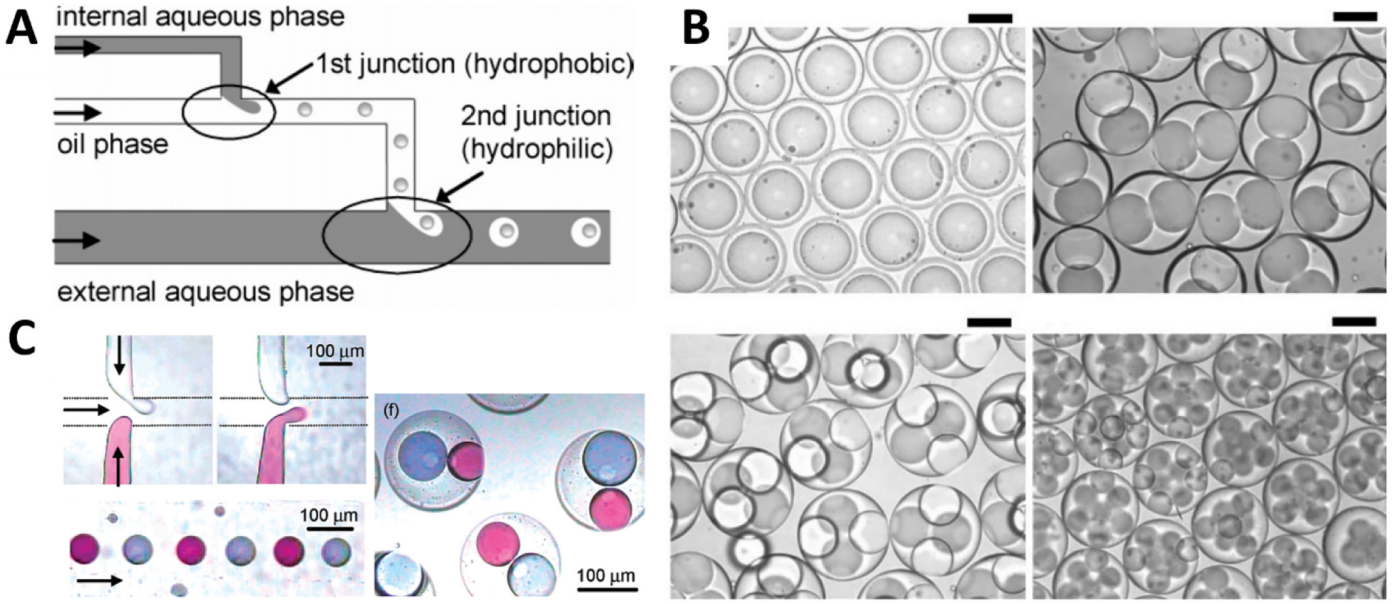

Fig. 5. Generation of double emulsions and core-shell particles in PDMS-based channels. (A) A scheme of double emulsions generated by a two-step emulsification in a double T-junction. (B) Double emulsions with controlled size and numbers of inner droplets. (C) Controlling the contents of inner droplets in double emulsions in a cross junction. Reproduced with permission from ref. [159] for (A, C) and [160] for (B). Copyright 2004 American Chemical Society and 2005 The Royal Society of Chemistry.

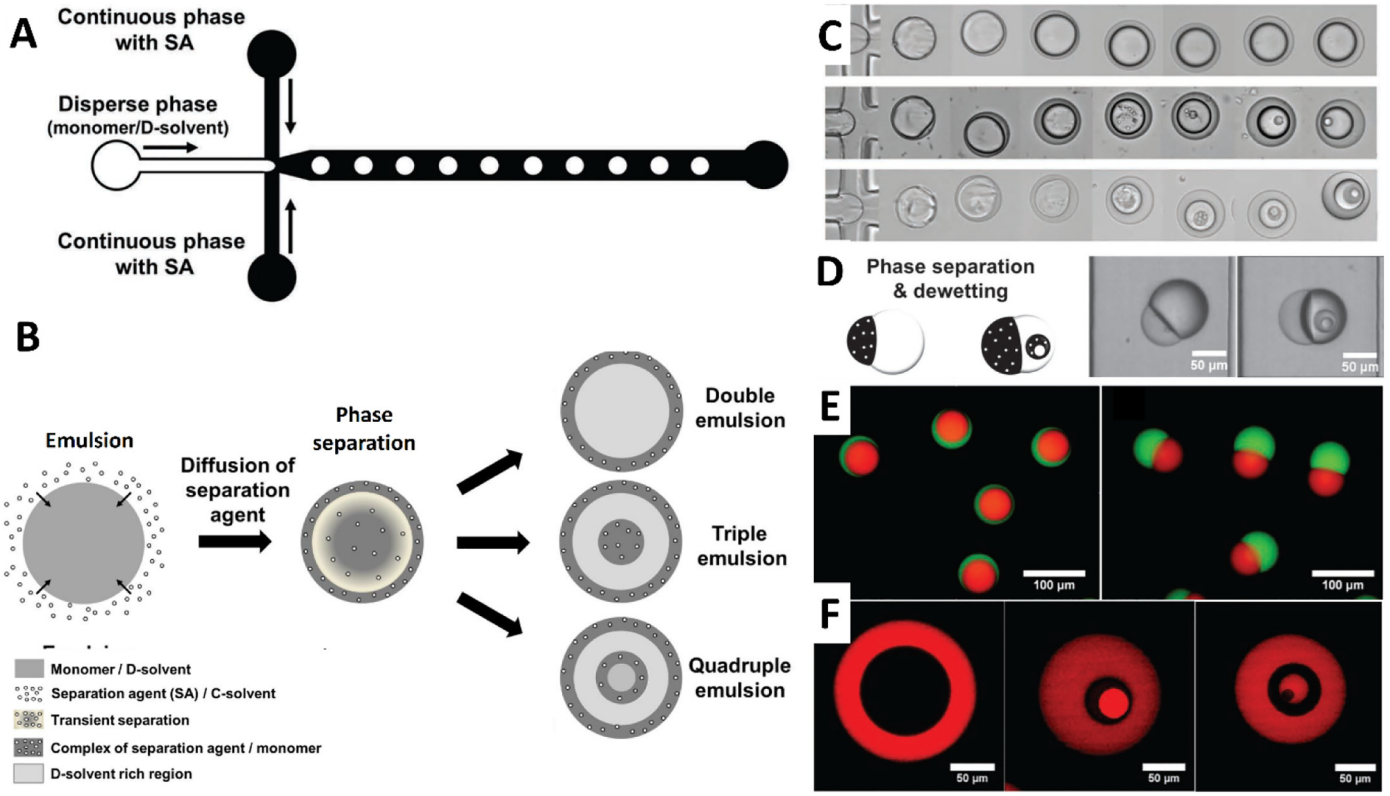

Fig. 6. Phase separation induced the formation of complex emulsions and their capability for selective encapsulation of cargo molecules. (A) A scheme showing the generation of complex emulsions by single emulsification within a simple microfluidic device. (B) A scheme of the evolution of single emulsions into complex emulsions induced by phase separation. (C) Sequential images showing the transformation of a single emulsion by phase separation to form a double (top), a triple (middle), and a quadruple emulsion (bottom). (D) A scheme (left) and optical micrographs (right) of the Janus double and Janus triple emulsions formed by an ensemble of phase separation and dewetting. (E) A fluorescent image showing that the hydrophilic (red) and hydrophobic (green) dyes were spontaneously introduced into each part of the double emulsion (left) and Janus emulsion (right). (F) CLSM images showing the selective encapsulation of hydrophobic dyes (red) into each shell region of the multiple emulsions. Reproduced with permission from ref. [119]. Copyright 2013 Wiley-VCH. (For interpretation of the references to color in this figure legend, the reader is referred to the web version of this article.)

materials. Alternatively, Utada et al. first demonstrated a glass capillary microfluidic device that generates double emulsions in a single step, facilitating not only precise control of the outer and inner droplet sizes but also the number of droplets encapsulated in each larger drop [112]. There are several approaches for producing complex emulsions, exploiting unique opportunities for increasing the functionality of particles by incorporating various additives, such as dyes in a model drug, magnetic nanoparticles, quantum dots and photonic crystals [125,139,164]. These approaches have also been utilized to design efficient carriers for the encapsulation of drugs, peptides, proteins and cells, which can be utilized in various biomedical applications [125,127–129,165–171].

Chu et al. reported the generation of triple emulsions with precisely controlled sizes and numbers of core droplets using multiple coflowing geometries in capillary microfluidic devices [172]. First, the innermost fluid was injected into the injection capillary and emulsified through the transition capillary by the middle fluid flowing in a co-axial direction. The resulting single emulsion was further emulsified by the outermost fluid to form a triple emulsion, as shown in Fig. 7A. The dimensions of the orifice and the flow rate of all the fluids are important parameters to control the size of the inner, middle and outer droplets. Depending on the parameters, a hierarchical level of multiple emulsions was formed, as shown in Fig. 7B. A novel microcapsule with thermosensitivity was formed by using complex emulsions, containing a photocurable NIPAm solution and W/O/W/O emulsions as a template in the outer aqueous layer. The generated pNIPAm particles exhibited highly controlled releasing characteristics depending on the temperature. At low temperatures, the hydrogel shells of the microcapsules retain water droplets containing oil droplets, while the shells shrink, break, and release at high temperatures, as shown in Fig. 7C. The results showed the possibility of using microfluidics to design new, highly engineered, and structured materials for controlled release of active substance. The microfluidic approach introduced so far allows for the formation of complex emulsions with uniformly controlled properties and superior control of the hydrodynamic parameters. However, this approach requires a complex design or a serial device consisting of a single drop generator. In addition, it is difficult to synchronize the frequency of droplet formation. An alternative route for forming a highly refined complex emulsion based on the first stage emulsion in a microfluidic device has been demonstrated by Kim et al. [173]. To form complex emulsions, a square capillary and two cylindrical capillaries are utilized. Briefly, two biphasic fluid streams (O_1/W_1, W_2/O_2) are introduced into each inlet and three interfaces are formed coaxially. O and W indicate oil phase and water phase, and 1 and 2 describe the biphasic fluids flowing into both outer channels, respectively. Meanwhile, the water phase (W_3), which is the innermost fluid, is injected into one end. These results demonstrate the formation of monodisperse quadruple emulsions in a single step, as shown in Fig. 7D and E. The results presented in this research are promising for various research areas, such as novel drug carriers, displays and microreactors with good process stability, simplicity and controllability.

Kim et al. also demonstrated the formation of temperature sensitive microgels composed of pNIPAm via a coflowing capillary microfluidic device and a subsequent in situ redox polymerization, as shown in Fig. 8A [125]. According to their report, they simply adjusted the microsphere size from 10 μm to 1000 μm by changing the flow rate.

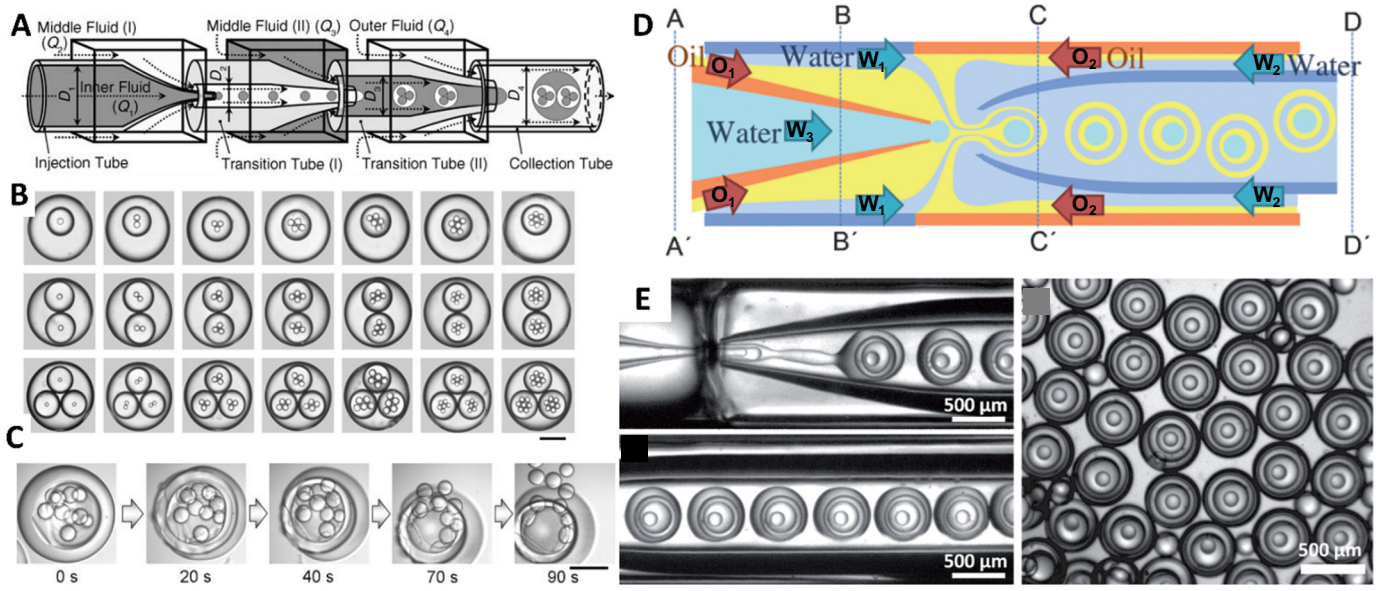

Fig. 7. Formation of highly complex emulsions via capillary-based microfluidic devices. (A) A scheme of the formation of complex triple emulsions by stepwise emulsification in the coflowing geometry of the microfluidic device. (B) Precisely controlled size and number of inner droplets in the triple emulsions. (C) Sequential micrographs showing the release of the oil and water droplets from thermosensitive microcapsules in response to the temperature of 50 °C. (D) A scheme presenting one-step formation of W/O/W/O/W quadruple emulsions via coflowing microfluidic devices. The fluid is composed of water-phases (W_1, W_2, and W_3) and oil phases (O_1 and O_2). (E) Optical images showing the formation of quadruple emulsions (left) and the highly uniform quadruple emulsions (right). Reproduced with permission from ref. [172,173]. Copyright 2007 and 2011 Wiley-VCH.

Additionally, they incorporated additives, such as polystyrene microparticles, quantum dots, and magnetic nanoparticles into the NIPAm microspheres by physical captures, as shown in Fig. 8B. Furthermore, the produced microspheres presented the 0.9 of thermoresponsive volumetric change as the temperature varied from 25 °C to 80 °C. This result shows that the microfluidic device can be used as a device to produce microgel particles containing small nanoparticles. As reported, it was used as a template to form Janus microspheres with strong water repelling properties [121]. An emulsion composed of photocurable resins with incorporated silica nanoparticles was formed via coflowing capillary-based microfluidic devices. The formed emulsion was photopolymerized by UV radiation, and then, wet-etched silica particles were used as the templates to form microspheres with microcavities. Then, the resultant microspheres were fluorinated, and it enabled the formation of superhydrophobic microspheres, as shown in Fig. 8C. The superhydrophobicity of the Janus microspheres derived from the fluorinated cavity structures was clearly demonstrated by handling large liquid water droplets stabilized by Janus superhydrophobic microspheres, as shown in Fig. 8D. The efficient method of forming monodispersed Janus microspheres based on the microfluidics enables the design path for superhydrophobic materials with highly uniform and unique properties, which cannot easily be generated by the conventional techniques [121].

Microparticles exhibiting optically unique characteristics have been recently reported [124]. The double emulsion encapsulating crystalline colloidal arrays (CCAs) were formed by a two-step coflowing emulsification. For instance, an inner phase, composed of an aqueous suspension of polystyrene nanoparticles (PS, 328 nm in diameter, 10 vol%

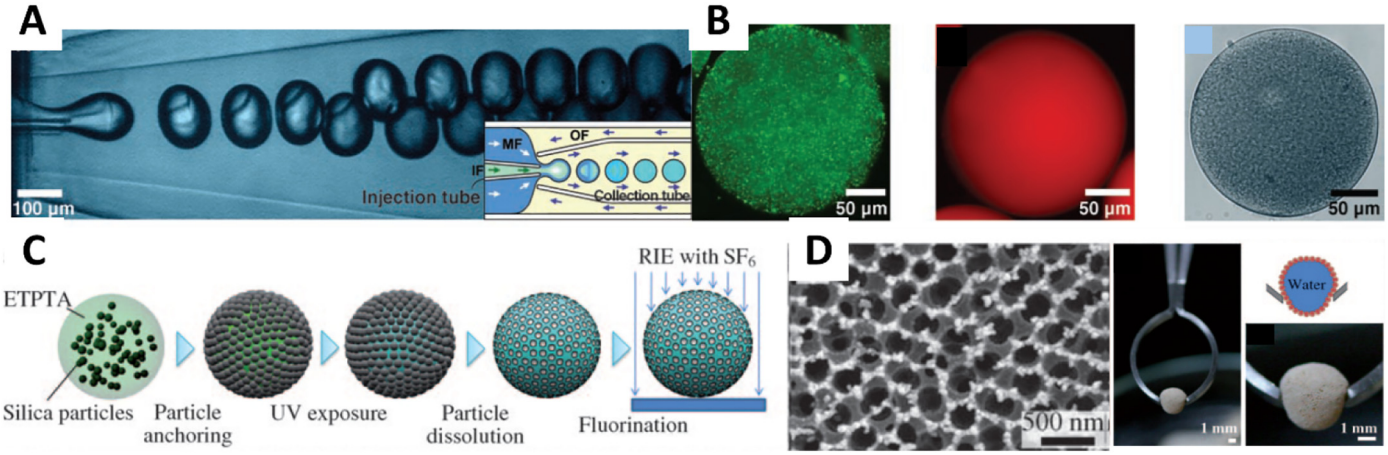

Fig. 8. Generation of functional microspheres via capillary-based microfluidic devices and their versatile applications as drug delivery systems and superhydrophobic Janus microspheres. (A) Thermoresponsive pNIPAm microspheres in a coflowing microfluidic device. (B) Composite materials that entrap fluorescent PS particles (left), quantum dots (middle), and magnetic particles (right). (C) A scheme presenting the sequence of forming superhydrophobic Janus microspheres via a coflowing microfluidic device and RIE etching and fluorination. (D) A scanning electron microscopy (SEM) image showing the microcavities on the surface of the Janus superhydrophobic microspheres (left) and their application of liquid marble handling (right). Reproduced with permission from ref. [125] for (A, B) and [121] for (C, D). Copyright 2007 and 2010 Wiley-VCH.

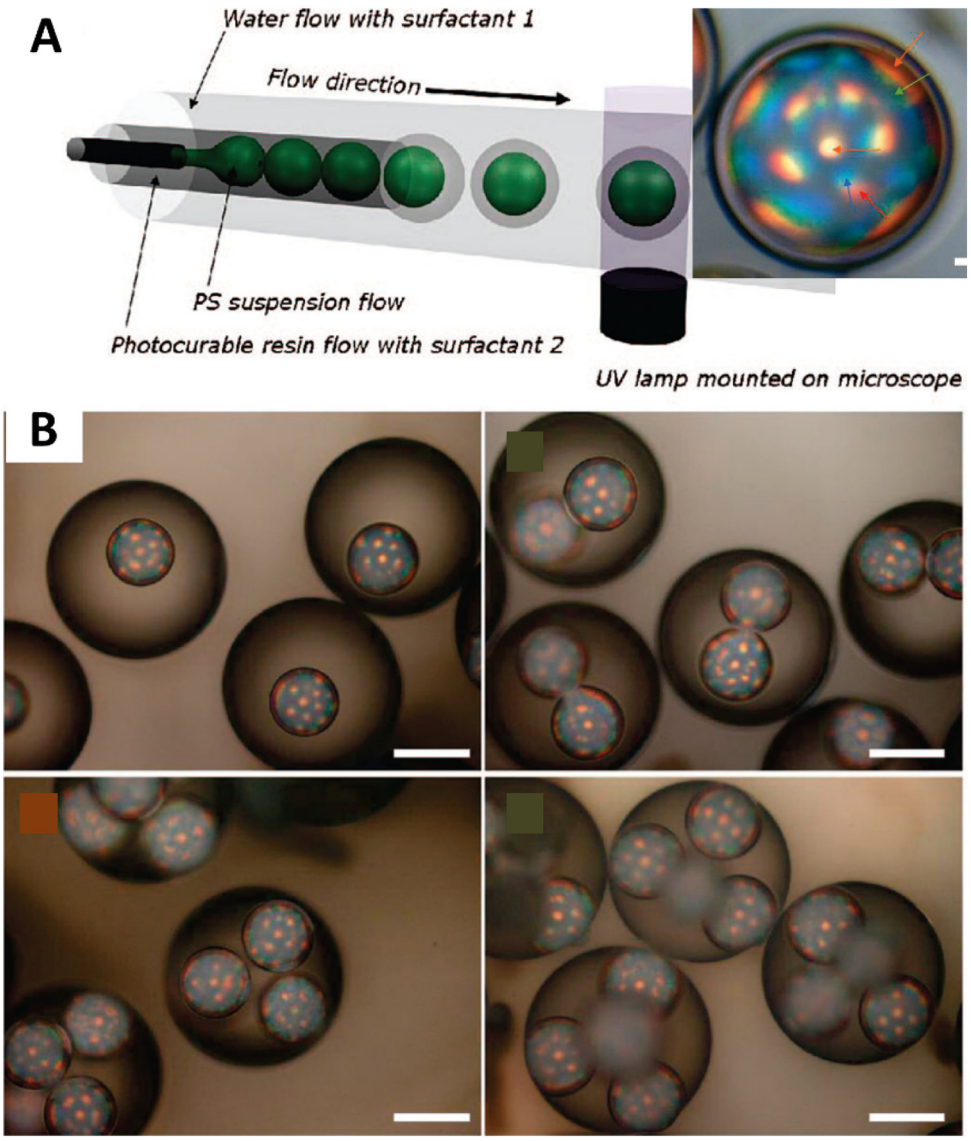

Fig. 9. Production of double emulsions and core-shell particles with controlled inner droplets by varying the flow rates of each fluid. (A) A scheme representing the encapsulation of crystalline colloidal arrays (CCAs) within microspheres after UV polymerization of double emulsions (inset: diffraction patterns of the core-shell particles). (B) Core-shell particles with a controllable number of inner cores within the CCAs. Reproduced with permission from ref. [124]. Copyright 2008 American Chemical Society.

particle loading), and the middle phase, containing a photocurable solution, were co-flowed and broken up into a W/O. Then, the resultant W/O emulsions further met a continuous phase, resulting in the formation of W/O/W emulsions containing PS nanoparticles. The double emulsions were UV-polymerized, forming microcapsules with CCAs, as shown in Fig. 9A. The number of inner-core containing CCAs of the core-shell particles is precisely controllable by varying the flow rates, as shown in Fig. 9B. According to their report, the generated capsules exhibited unique patterns of diffraction that have not been achieved in conventional film type arrays. In addition, improved stability of the CCAs was achieved by the encapsulated environments' ability to reduce the permeability of the ions and molecules whose encapsulated environment negatively impacts the CCAs compared to the conventional technology.

Lorenceau et al. demonstrated the formation of double emulsions and polymersomes via glass capillary-based coflowing microfluidic devices [126]. The device consisted of two cylindrical capillaries facing each other in a square capillary. The innermost fluid (water) was injected through a cylindrical capillary, and the middle fluid (a diblock copolymer in a mixture of THF-Toluene cosolvent) was introduced between the capillary used for the innermost fluid and the square capillary. The outermost fluid (glycerol/water mixture) was simultaneously injected into the opposite side of the capillary wall. In this state, polymersomes were formed by self-assembly of vesicles within the middle layer, which is driven by the slow evaporation of the cosolvents, as shown in Fig. 10A. The formed polymersomes feature the controllable releasing of the inner water fluids by the osmotic pressure difference. When sucrose was added to the polymersome-dispersed solution, the polymersomes shrank due to the osmotic pressure difference between the inner and outer environments. This results in the release of water from the polymersomes, indicating their potential application as microcapsules with stimuli-responsive releasing kinetics, as shown in Fig. 10B.

One of the emerging issues for the encapsulation of active materials is high-efficiency retainment while stably storing cargo materials. In particular, it is very challenging to retain high-valued substances, for instance, densely encapsulated fragrances, due to their volatility [123,174–179]. Recently, Choi et al. presented polymeric

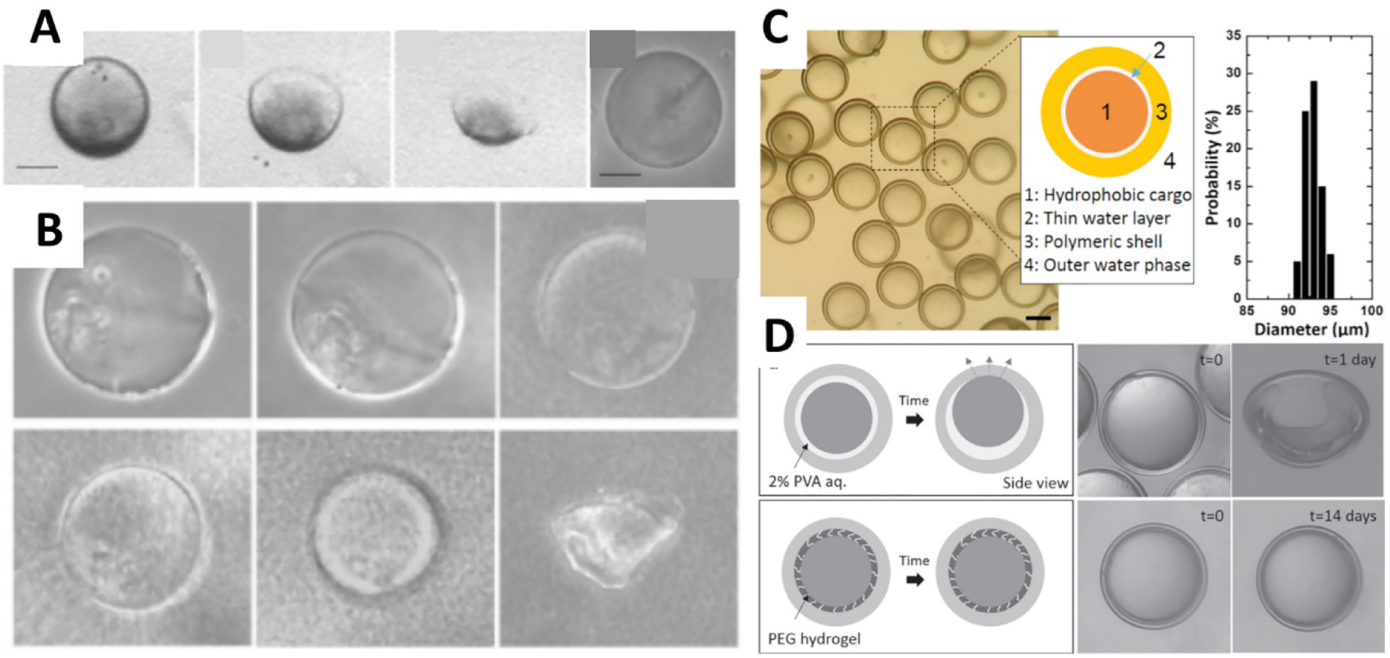

Fig. 10. Generation of double and triple emulsions, polymersomes and microcapsules via glass capillary-based coflowing microfluidics. (A) Sequential micrographs showing the formation of polymersomes from double emulsions by solvent evaporation from the mixtures in the middle layer; as the solvents evaporated, the layers became transparent (three images from the left). A phase contrast image showing the polymersomes (right). (B) The shrinkage of the polymersomes induced by the osmotic pressure difference between the external and internal microenvironments. Reproduced with permission from ref. [126] for (A, B). Copyright 2005 American Chemical Society. (C) An optical micrograph and quantitative analysis showing the uniformity of the monodisperse microcapsules with ultrathin water layers. (D) The collapsing of the microcapsules due to diffusion out of the encapsulated hydrophobic cargo (top) and the stabilized retention of the hydrophobic cargo within the microcapsules by the hydrogel acting as a diffusion barrier (bottom). Reproduced with permission from ref. [123] for (C, D). Copyright 2016 Wiley-VCH.

microcapsules featuring a high encapsulation efficiency for volatile hydrophobic cargo formed by the polymerization of triple emulsions including an ultrathin water layer [123]. Monodisperse triple emulsions (O/W/O/W) with an ultrathin water layer were generated by one-step emulsification in flow-focusing glass capillary devices. The ultrathin water layer provided a high encapsulation efficiency for the hydrophobic cargo, as shown in Fig. 10C. Moreover, the retention of hydrophobic cargo could be improved by the formation of a hydrogel layer after solidifying the hydrogel precursor in the ultrathin water layer. The hydrophobic cargo in the microcapsules without the hydrogel layer easily leaked within 1 day and showed buckling of the microcapsule. In contrast, the microcapsules with the hydrogel layer showed high retainability for the cargo without any changes in the microcapsule for 14 days, as shown in Fig. 10D. The unique features of the hydrophobic cargo surrounded by the water thin layer enable a high encapsulation efficiency and enhanced retention, indicating the ability of microfluidics to form finely tuned functional materials with desirable characteristics.

Nisisako et al. reported the formation of Janus microspheres with asymmetric electrical properties using a y-shaped etched glass microfluidic device with a precisely controlled capillary number (*Ca*) [120]. Carbon black and titanium oxides were used as the dispersed phase. Initiator added monomers were used for the continuous phase, and they are formed into bicolored Janus emulsions. The resultant templates were thermal-polymerized to yield monodisperse Janus microspheres with two discrete parts, as shown in Fig. 11A and B. According to their report, the *Ca* was one of the most important factors to produce bicolored emulsions continuously due to the viscoelastic properties of the polymeric solution. At low *Ca* values with a constant Q_d, the Janus emulsion formations are stable, while the polydisperse emulsions were formed due to unstable breakage at high *Ca* values. They noted that the formation of the bicolored Janus emulsion was unstable, while the two prepolymeric solutions flow with different viscosities at the same rate. The Janus microspheres formed with different electromagnetic properties were used for display technology by binary manipulation between black and white, depending on the applied electric field, as shown in Fig. 11C.

The complex emulsions with ordered internal structures were formed by phase separation of a ternary mixture, as recently evidenced by Haase and Brujic [122]. Briefly, a disperse phase consisting of oil, a polar solvent and water stream was injected into an aqueous continuous phase through a capillary to initiate dripping. During the formation of the droplets, mass transfer occurred between the two phases due to diffusion out of the oil and polar solvent, with simultaneous diffusion in toward the disperse phase of the aqueous phase containing the water with the surfactant. This process changes the composition of the droplets and subsequently induces spinodal decomposition or nucleation and growth at nonequilibrium conditions. Subsequently, coalescence occurred, and these cycles are repeated until the system reaches the thermodynamically stable point and it forms a complex emulsion. Depending on the initial composition of the mixtures, the number of cycles can be manipulated to change the final form of the complex emulsion, as shown in Fig. 12A. The approach was utilized to generate PMMA microcapsules with the capability for selective cargo loading and unilamellar vesicles. Furthermore, droplets with complex internal structures could be produced using lipids and the coalesce of oil layers upon droplet contact with subsequent evaporation of the oil from the outer layer, as shown in Fig. 12B. As shown Fig. 12C, these multiple droplets containing 2, 4, or 6 droplets can also have complex internal structure, and it can be used to prepare particles with complex topologies.

5. Conclusion and outlook

In this review, the basic and various flow shapes and structures, and representative control factors of microfluidics were surveyed and summarized. The results of studies on the synthesis of functional materials were discussed, which were carried out using microfluidic devices designed in various forms. Through this series of processes, we

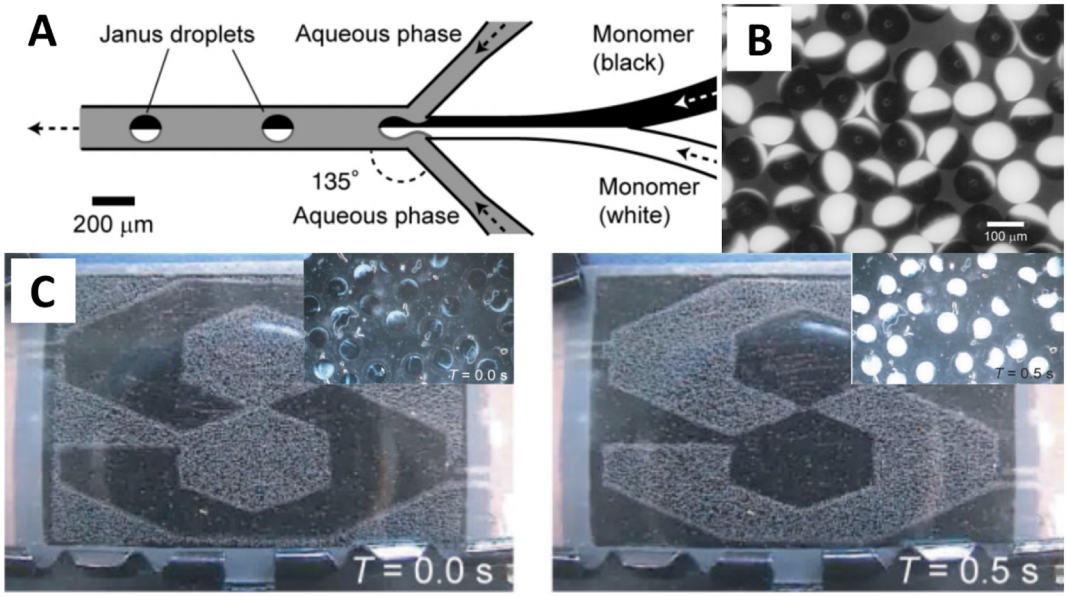

Fig. 11. Formation of hybrid Janus microspheres by controlling the capillary number in glass microchannels. (A) Janus microspheres formed via a y-shaped microchannel. (B) An optical micrograph showing monodisperse microspheres with two discrete parts: carbon black (black) and titanium oxide (white). (C) Actuation of a display due to the reorientation of Janus microparticles between black and white as a response to the applied electrical field; inset images show enlarged images of the Janus microspheres displaying either black or white depending on the direction. Reproduced with permission from ref. [120] for (A–C). Copyright 2009 and 2006 Wiley-VCH.

were able to reach the following conclusions. Microfluidics can provide excellent platforms for the synthesis of functional materials, including polymeric and inorganic materials, with sizes ranging from nanometers to micrometers. Furthermore, through the microfluidic device, it was found that not only could the fine particles of well-controlled characteristics be produced, which were difficult to secure by the existing chemical synthesis, but also functional fine particles with new physicochemical properties could be produced. The most distinctive features were in the properties of materials made using microfluidics devices. Various microparticles prepared using the microfluidic devices presented better performance than particles prepared through conventional synthetic methods. Furthermore, these unique features can be applied to a wide variety of applications and it is believed that this could provide a platform for a strong raw material for research in the fields of medicine, optics, and electronics, including basic science research. Consequently, though the synthesis of functional materials using microfluidics is in the research stage currently, we will be able to design the functional materials and microfluidic systems in the near the future, and it is believed that this will greatly contribute to opening the era of new materials.

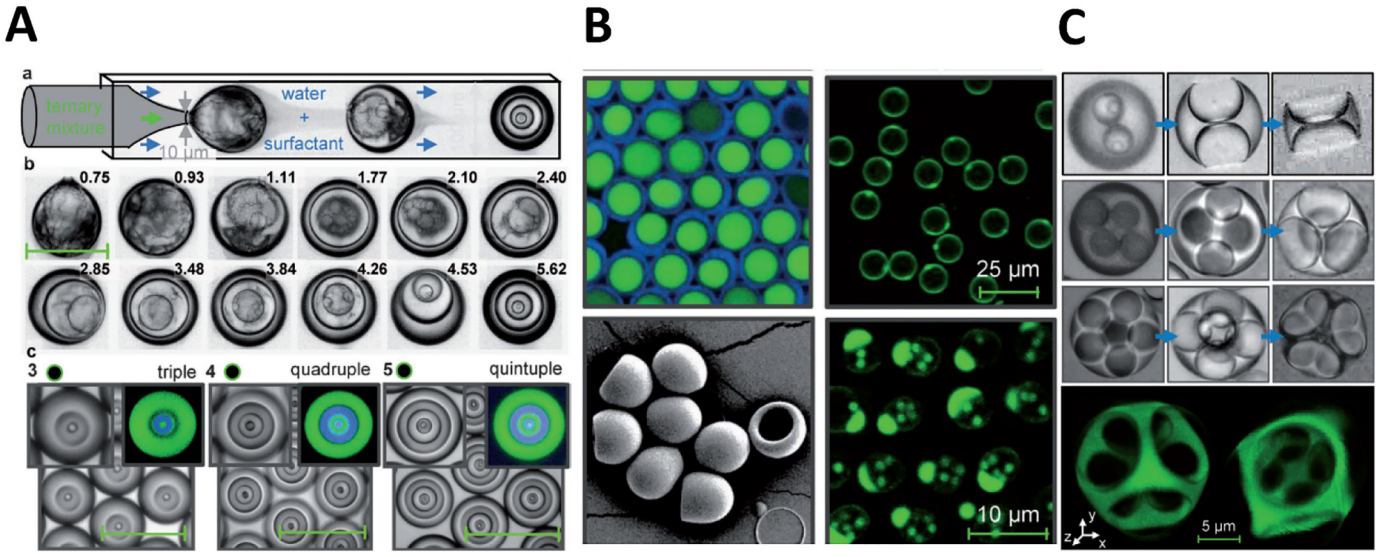

Fig. 12. Formation of complex emulsions through phase separation in a glass capillary-based coflowing microfluidic device and their application to form capsules, vesicles and droplets with highly ordered internal structures. (A) A scheme presenting the formation (top) and evolution (middle) of complex emulsions (bottom), such as double, triple, quadruple and quintuple emulsions. (B) Fluorescent micrographs showing PMMA microcapsules with the selective encapsulation of distinctive dyes (left top), and their collapsed structures are shown in the SEM image (left, bottom). The fluorescent images showing the unilamellar vesicles (right top) and the vesicles encapsulating 1 μm colloids (right, bottom). (C) Varying shapes of the complex emulsions with different numbers of water droplets (N = 2: top, N = 4: middle, and N = 6: bottom) and ordered inner structures in the final state (fluorescent image; green). Reproduced with permission from ref. [122]. Copyright 2014 Wiley-VCH. (For interpretation of the references to color in this figure legend, the reader is referred to the web version of this article.)

Acknowledgement

This research was supported by Next-Generation Information Computing Development Program (NRF-2015M1A5A1037054) and Global Research Laboratory (NRF-2015K1A1A2033054) through the National Research Foundation of Korea (NRF), funded by the Ministry of Science and ICT.

References

[1] B.G. Chung, K.H. Lee, A. Khademhosseini, S.H. Lee, Microfluidic fabrication of microengineered hydrogels and their application in tissue engineering, Lab Chip 12 (1) (2012) 45–59.
[2] A.L. Thangawng, P.B. Howell, C.M. Spillmann, J. Naciri, F.S. Ligler, UV polymerization of hydrodynamically shaped fibers, Lab Chip 11 (6) (2011) 1157–1160.
[3] D. Velasco, E. Tumarkin, E. Kumacheva, Microfluidic encapsulation of cells in polymer microgels, Small 8 (11) (2012) 1633–1642.
[4] V. Wood, M.J. Panzer, J.M. Caruge, J.E. Halpert, M.G. Bawendi, V. Bulovic, Air-stable operation of transparent, colloidal quantum dot based LEDs with a unipolar device architecture, Nano Lett. 10 (1) (2010) 24–29.
[5] R. Rhodes, S. Asghar, R. Krakow, M. Horie, Z.J. Wang, M.L. Turner, B.R. Saunders, Hybrid polymer solar cells: from the role colloid science could play in bringing deployment closer to a study of factors affecting the stability of non-aqueous ZnO dispersions, Colloids Surf. A Physicochem. Eng. Asp. 343 (1–3) (2009) 50–56.
[6] S.H. Kim, S.Y. Lee, S.M. Yang, G.R. Yi, Self-assembled colloidal structures for photonics, NPG Asia Mater. 3 (1) (2011) 25–33.
[7] S. Sacanna, D.J. Pine, Shape-anisotropic colloids: building blocks for complex assemblies, Curr. Opin. Colloid Interface Sci. 16 (2) (2011) 96–105.
[8] J. Pardeike, A. Hommoss, R.H. Muller, Lipid nanoparticles (SLN, NLC) in cosmetic and pharmaceutical dermal products, Int. J. Pharm. 366 (1–2) (2009) 170–184.
[9] B. Comiskey, J.D. Albert, H. Yoshizawa, J. Jacobson, An electrophoretic ink for all-printed reflective electronic displays, Nature 394 (6690) (1998) 253–255.
[10] S.W. Oh, C.W. Kim, H.J. Cha, U. Pal, Y.S. Kang, Encapsulated-dye all-organic charged colored ink nanoparticles for electrophoretic image display, Adv. Mater. 21 (48) (2009) 4987–4991.
[11] R. Stanway, Smart fluids: current and future developments, Mater. Sci. Technol. 20 (8) (2004) 931–939.
[12] C. Grosse, A.V. Delgado, Dielectric dispersion in aqueous colloidal systems, Curr. Opin. Colloid Interface Sci. 15 (3) (2010) 145–159.
[13] R.C. Nagarwal, S. Kant, P.N. Singh, P. Maiti, J.K. Pandit, Polymeric nanoparticulate system: a potential approach for ocular drug delivery, J. Control. Release 136 (1) (2009) 2–13.
[14] S. Gouin, Microencapsulation: industrial appraisal of existing technologies and trends, Trends Food Sci. Technol. 15 (7–8) (2004) 330–347.
[15] J.C. De La Vega, P. Elischer, T. Schneider, U.O. Hafeli, Uniform polymer microspheres: monodispersity criteria, methods of formation and applications, Nanomedicine 8 (2) (2013) 265–285.
[16] T. Kawakatsu, Y. Kikuchi, M. Nakajima, Regular-sized cell creation in microchannel emulsification by visual microprocessing method, J. Am. Oil Chem. Soc. 74 (3) (1997) 317–321.
[17] T. Nakashima, M. Shimizu, M. Kukizaki, Particle control of emulsion by membrane emulsification and its applications, Adv. Drug Deliv. Rev. 45 (1) (2000) 47–56.
[18] T. Nakashima, M. Shimizu, M. Kukizaki, Membrane emulsification by microporous glass, Key Eng. Mater. (1992) 513–516.
[19] A.M. Ganan-Calvo, Generation of steady liquid microthreads and micron-sized monodisperse sprays in gas streams, Phys. Rev. Lett. 80 (2) (1998) 285–288.
[20] T.G. Mason, J. Bibette, Shear rupturing of droplets in complex fluids, Langmuir 13 (17) (1997) 4600–4613.
[21] P. Perrin, Amphiphilic copolymers: a new route to prepare ordered monodisperse emulsions, Langmuir 14 (21) (1998) 5977–5979.
[22] H. Song, D.L. Chen, R.F. Ismagilov, Reactions in droplets in microflulidic channels, Angew. Chem. Int. Ed. 45 (44) (2006) 7336–7356.
[23] A.B. Theberge, F. Courtois, Y. Schaerli, M. Fischlechner, C. Abell, F. Hollfelder, W.T.S. Huck, Microdroplets in microfluidics: an evolving platform for discoveries in chemistry and biology, Angew. Chem. Int. Ed. 49 (34) (2010) 5846–5868.
[24] G.M. Whitesides, The origins and the future of microfluidics, Nature 442 (7101) (2006) 368–373.
[25] H.A. Stone, A.D. Stroock, A. Ajdari, Engineering flows in small devices: microfluidics toward a lab-on-a-chip, Annu. Rev. Fluid Mech. 36 (2004) 381–411.
[26] G.F. Christopher, S.L. Anna, Microfluidic methods for generating continuous droplet streams, J. Phys. D. Appl. Phys. 40 (19) (2007) R319–R336.
[27] T.M. Squires, S.R. Quake, Microfluidics: fluid physics at the nanoliter scale, Rev. Mod. Phys. 77 (3) (2005) 977–1026.
[28] C.X. Zhao, A.P.J. Middelberg, Two-phase microfluidic flows, Chem. Eng. Sci. 66 (7) (2011) 1394–1411.
[29] R. Seemann, M. Brinkmann, T. Pfohl, S. Herminghaus, Droplet based microfluidics, Rep. Prog. Phys. 75 (1) (2012) 016601–016642.
[30] C.N. Baroud, F. Gallaire, R. Dangla, Dynamics of microfluidic droplets, Lab Chip 10 (16) (2010) 2032–2045.
[31] F.Y. Ushikubo, F.S. Birribilli, D.R.B. Oliveira, R.L. Cunha, Y- and T-junction microfluidic devices: effect of fluids and interface properties and operating conditions, Microfluid. Nanofluid. 17 (4) (2014) 711–720.
[32] M.C. Jullien, M.J.T.M. Ching, C. Cohen, L. Menetrier, P. Tabeling, Droplet breakup in microfluidic T-junctions at small capillary numbers, Phys. Fluids 21 (7) (2009).
[33] L. Rayleigh, XVI. On the instability of a cylinder of viscous liquid under capillary force, Lond. Edinb. Dublin Philos. Mag. J. Sci. 34 (207) (1892) 145–154.
[34] J.D. Tice, H. Song, A.D. Lyon, R.F. Ismagilov, Formation of droplets and mixing in multiphase microfluidics at low values of the Reynolds and the capillary numbers, Langmuir 19 (22) (2003) 9127–9133.
[35] A. Gupta, R. Kumar, Flow regime transition at high capillary numbers in a microfluidic T-junction: viscosity contrast and geometry effect, Phys. Fluids 22 (12) (2010) 122001–122011.
[36] S.L. Anna, N. Bontoux, H.A. Stone, Formation of dispersions using “flow focusing” in microchannels, Appl. Phys. Lett. 82 (3) (2003) 364–366.
[37] W. Lee, L.M. Walker, S.L. Anna, Role of geometry and fluid properties in droplet and thread formation processes in planar flow focusing, Phys. Fluids 21 (3) (2009) 032103–032116.
[38] W.-L. Ong, J. Hua, B. Zhang, T.-Y. Teo, J. Zhuo, N.-T. Nguyen, N. Ranganathan, L. Yobas, Experimental and computational analysis of droplet formation in a high-performance flow-focusing geometry, Sensors Actuators A Phys. 138 (1) (2007) 203–212.
[39] S. van der Graaf, T. Nisisako, C.G.P.H. Schroen, R.G.M. van der Sman, R.M. Boom, Lattice Boltzmann simulations of droplet formation in a T-shaped microchannel, Langmuir 22 (9) (2006) 4144–4152.
[40] A. Gupta, S.M.S. Murshed, R. Kumar, Droplet formation and stability of flows in a microfluidic T-junction, Appl. Phys. Lett. 94 (16) (2009).
[41] M.M. Dupin, I. Halliday, C.M. Care, Simulation of a microfluidic flow-focusing device, Phys. Rev. E 73 (5) (2006).
[42] L. Wu, M. Tsutahara, L.S. Kim, M. Ha, Three-dimensional lattice Boltzmann simulations of droplet formation in a cross-junction microchannel, Int. J. Multiphase Flow 34 (9) (2008) 852–864.
[43] D.R. Link, S.L. Anna, D.A. Weitz, H.A. Stone, Geometrically mediated breakup of drops in microfluidic devices, Phys. Rev. Lett. 92 (5) (2004).
[44] P. Garstecki, M.J. Fuerstman, H.A. Stone, G.M. Whitesides, Formation of droplets and bubbles in a microfluidic T-junction - scaling and mechanism of break-up, Lab Chip 6 (3) (2006) 437–446.
[45] J.K. Nunes, S.S.H. Tsai, J. Wan, H.A. Stone, Dripping and jetting in microfluidic multiphase flows applied to particle and fibre synthesis, J. Phys. D. Appl. Phys. 46 (11) (2013) 114002–114021.
[46] M. Rosoff, The nature of microemulsions, Progress in Surface and Membrane Science, Elsevier, 1978, pp. 405–477.
[47] M. Bourrel, A. Graciaa, R.S. Schechter, W.H. Wade, The relation of emulsion stability to phase behavior and interfacial tension of surfactant systems, J. Colloid Interface Sci. 72 (1) (1979) 161–163.
[48] S.L. Holt, Microemulsions: a contemporary overview, J. Dispers. Sci. Technol. 1 (4) (1980) 423–464.
[49] S.E. Friberg, Microemulsions, J. Dispers. Sci. Technol. 6 (3) (1985) 317–337.
[50] M.-J. Schwuger, K. Stickdorn, R. Schomaecker, Microemulsions in technical processes, Chem. Rev. 95 (4) (1995) 849–864.
[51] P. Kumar, K.L. Mittal, Handbook of Microemulsion Science and Technology, CRC press, 1999.
[52] W. Hou, J. Xu, Surfactant-free microemulsions, Curr. Opin. Colloid Interface Sci. 25 (2016) 67–74.
[53] A.S. Utada, A. Fernandez-Nieves, H.A. Stone, D.A. Weitz, Dripping to jetting transitions in coflowing liquid streams, Phys. Rev. Lett. 99 (9) (2007) 094502–094505.
[54] A.R. Abate, A. Poitzsch, Y. Hwang, J. Lee, J. Czerwinska, D.A. Weitz, Impact of inlet channel geometry on microfluidic drop formation, Phys. Rev. E 80 (2) (2009) 026310–026314.
[55] P. Guillot, A. Colin, A. Ajdari, Stability of a jet in confined pressure-driven biphasic flows at low Reynolds number in various geometries, Phys. Rev. E 78 (1) (2008) 016307–016319.
[56] M.A. Herrada, A.M. Ganan-Calvo, P. Guillot, Spatiotemporal instability of a confined capillary jet, Phys. Rev. E 78 (4) (2008) 046312–046318.
[57] H. Gu, M.H.G. Duits, F. Mugele, Droplets formation and merging in two-phase flow microfluidics, Int. J. Mol. Sci. 12 (4) (2011) 2572–2597.
[58] T. Thorsen, R.W. Roberts, F.H. Arnold, S.R. Quake, Dynamic pattern formation in a vesicle-generating microfluidic device, Phys. Rev. Lett. 86 (18) (2001) 4163–4166.
[59] G.F. Christopher, N.N. Noharuddin, J.A. Taylor, S.L. Anna, Experimental observations of the squeezing-to-dripping transition in T-shaped microfluidic junctions, Phys. Rev. E 78 (3) (2008).
[60] A.R. Abate, A. Poitzsch, Y. Hwang, J. Lee, J. Czerwinska, D.A. Weitz, Impact of inlet channel geometry on microfluidic drop formation, Phys. Rev. E 80 (2) (2009).
[61] M.L.J. Steegmans, K.G.P.H. Schroen, R.M. Boom, Characterization of emulsification at flat microchannel Y junctions, Langmuir 25 (6) (2009) 3396–3401.
[62] A. Gupta, R. Kumar, Effect of geometry on droplet formation in the squeezing regime in a microfluidic T-junction, Microfluid. Nanofluid. 8 (6) (2010) 799–812.
[63] D. Malsch, N. Gleichmann, M. Kielpinski, G. Mayer, T. Henkel, D. Mueller, V. van Steijn, C.R. Kleijn, M.T. Kreutzer, Dynamics of droplet formation at T-shaped nozzles with elastic feed lines, Microfluid. Nanofluid. 8 (4) (2010) 497–507.
[64] K. Wang, Y.C. Lu, J. Tan, B.D. Yang, G.S. Luo, Generating gas/liquid/liquid three-phase microdispersed systems in double T-junctions microfluidic device, Microfluid. Nanofluid. 8 (6) (2010) 813–821.
[65] T. Glawdel, C. Elbuken, C.L. Ren, Droplet formation in microfluidic T-junction generators operating in the transitional regime. II. Modeling, Phys. Rev. E 85 (1) (2012).
[66] R. Lin, J.S. Fisher, M.G. Simon, A.P. Lee, Novel on-demand droplet generation for selective fluid sample extraction, Biomicrofluidics 6 (2) (2012) 024103.

[67] A.R. Abate, D.A. Weitz, Air-bubble-triggered drop formation in microfluidics, Lab Chip 11 (10) (2011) 1713–1716.
[68] L. Ménétrier-Deremble, P. Tabeling, Droplet breakup in microfluidic junctions of arbitrary angles, Phys. Rev. E 74 (3) (2006) 035303.
[69] M. Rhee, P. Liu, R.J. Meagher, Y.K. Light, A.K. Singh, Versatile on-demand droplet generation for controlled encapsulation, Biomicrofluidics 8 (3) (2014) 034112.
[70] Y. Ding, X.C. i Solvas, "V-junction": a novel structure for high-speed generation of bespoke droplet flows, Analyst 140 (2) (2015) 414–421.
[71] U. Tangen, A. Sharma, P. Wagler, J.S. McCaskill, On demand nanoliter-scale microfluidic droplet generation, injection, and mixing using a passive microfluidic device, Biomicrofluidics 9 (1) (2015) 014119.
[72] L. Wang, Y. Zhang, L. Cheng, Magic microfluidic T-junctions: valving and bubbling, Chaos, Solitons Fractals 39 (4) (2009) 1530–1537.
[73] K. Khoshmanesh, A. Almansouri, H. Albloushi, P. Yi, R. Soffe, K. Kalantar-Zadeh, A multi-functional bubble-based microfluidic system, Sci. Rep. 5 (2015).
[74] V. van Steijn, C.R. Kleijn, M.T. Kreutzer, Flows around confined bubbles and their importance in triggering pinch-off, Phys. Rev. Lett. 103 (21) (2009) 214501–214504.
[75] P. Guillot, A. Colin, Stability of parallel flows in a microchannel after a T junction, Phys. Rev. E 72 (6) (2005) 066301–066304.
[76] J.D. Tice, A.D. Lyon, R.F. Ismagilov, Effects of viscosity on droplet formation and mixing in microfluidic channels, Anal. Chim. Acta 507 (1) (2004) 73–77.
[77] S.L. Anna, N. Bontoux, H.A. Stone, Formation of dispersions using "flow focusing" in microchannels, Appl. Phys. Lett. 82 (3) (2003) 364–366.
[78] S.L. Anna, H.C. Mayer, Microscale tipstreaming in a microfluidic flow focusing device, Phys. Fluids 18 (12) (2006) 121512–121521.
[79] T. Cubaud, T.G. Mason, Capillary threads and viscous droplets in square microchannels, Phys. Fluids 20 (5) (2008) 053302–053313.
[80] L. Yobas, S. Martens, W.L. Ong, N. Ranganathan, High-performance flow-focusing geometry for spontaneous generation of monodispersed droplets, Lab Chip 6 (8) (2006) 1073–1079.
[81] K.J. Humphry, A. Ajdari, A. Fernandez-Nieves, H.A. Stone, D.A. Weitz, Suppression of instabilities in multiphase flow by geometric confinement, Phys. Rev. E 79 (5) (2009) 056310–056314.
[82] J. Berthier, S. Le Vot, P. Tiquet, N. David, D. Lauro, P.Y. Benhamou, F. Rivera, Highly viscous fluids in pressure actuated flow focusing devices, Sensors Actuators A Phys. 158 (1) (2010) 140–148.
[83] D. Funfschilling, H. Debas, H.Z. Li, T.G. Mason, Flow-field dynamics during droplet formation by dripping in hydrodynamic-focusing microfluidics, Phys. Rev. E 80 (1) (2009) 015301–015304.
[84] F. Lapierre, N. Wu, Y. Zhu, Influence of flow rate on the droplet generation process in a microfluidic chip, Smart Nano-Micro Materials and Devices, International Society for Optics and Photonics, 2011(pp. 82040H-82046H).
[85] W. Lee, L.M. Walker, S.L. Anna, Impact of viscosity ratio on the dynamics of droplet breakup in a microfluidic flow focusing device, The XV International Congress on Rheology: The Society of Rheology 80th Annual Meeting, AIP Publishing, 2008, pp. 994–996.
[86] W.L. Ong, J.S. Hua, B.L. Zhang, T.Y. Teo, J.L. Zhuo, N.T. Nguyen, N. Ranganathan, L. Yobas, Experimental and computational analysis of droplet formation in a high-performance flow-focusing geometry, Sensors Actuators A Phys. 138 (1) (2007) 203–212.
[87] L. Peng, M. Yang, S.S. Guo, W. Liu, X.Z. Zhao, The effect of interfacial tension on droplet formation in flow-focusing microfluidic device, Biomed. Microdevices 13 (3) (2011) 559–564.
[88] P. Garstecki, H.A. Stone, G.M. Whitesides, Mechanism for flow-rate controlled breakup in confined geometries: a route to monodisperse emulsions, Phys. Rev. Lett. 94 (16) (2005) 164501–164504.
[89] Z.H. Nie, M.S. Seo, S.Q. Xu, P.C. Lewis, M. Mok, E. Kumacheva, G.M. Whitesides, P. Garstecki, H.A. Stone, Emulsification in a microfluidic flow-focusing device: effect of the viscosities of the liquids, Microfluid. Nanofluid. 5 (5) (2008) 585–594.
[90] P.B. Umbanhowar, V. Prasad, D.A. Weitz, Monodisperse emulsion generation via drop break off in a coflowing stream, Langmuir 16 (2) (2000) 347–351.
[91] C. Cramer, P. Fischer, E.J. Windhab, Drop formation in a co-flowing ambient fluid, Chem. Eng. Sci. 59 (15) (2004) 3045–3058.
[92] W.J. Jeong, J.Y. Kim, J. Choo, E.K. Lee, C.S. Han, D.J. Beebe, G.H. Seong, S.H. Lee, Continuous fabrication of biocatalyst immobilized microparticles using photopolymerization and immiscible liquids in microfluidic systems, Langmuir 21 (9) (2005) 3738–3741.
[93] A.S. Utada, A. Fernandez-Nieves, J.M. Gordillo, D.A. Weitz, Absolute instability of a liquid jet in a coflowing stream, Phys. Rev. Lett. 100 (1) (2008) 014502–014505.
[94] P. Guillot, A. Colin, A.S. Utada, A. Ajdari, Stability of a jet in confined pressure-driven biphasic flows at low Reynolds numbers, Phys. Rev. Lett. 99 (10) (2007) 104502–104505.
[95] E. Castro-Hernandez, V. Gundabala, A. Fernandez-Nieves, J.M. Gordillo, Scaling the drop size in coflow experiments, New J. Phys. 11 (2009) 075021–075038.
[96] M.L. Cordero, F. Gallaire, C.N. Baroud, Quantitative analysis of the dripping and jetting regimes in co-flowing capillary jets, Phys. Fluids 23 (9) (2011) 094111–094119.
[97] R. Lord, On the instability of jets, Proc. Lond. Math. Soc. s1–10 (1) (1878) 4–13.
[98] A.S. Utada, A. Fernandez-Nieves, H.A. Stone, D.A. Weitz, Dripping to jetting transitions in coflowing liquid streams, Phys. Rev. Lett. 99 (9) (2007).
[99] J. Plateau, J. Plateau Acad. Sci. Bruxelles Mém. 23 (5) (1849) (Acad. Sci. Bruxelles Mém. 23 (1849) 5).
[100] S. Leib, M. Goldstein, Convective and absolute instability of a viscous liquid jet, Phys. Fluids 29 (4) (1986) 952–954.
[101] W. Vansaarloos, Front propagation into unstable states. 2. Linear versus nonlinear marginal stability and rate of convergence, Phys. Rev. A 39 (12) (1989) 6367–6390.
[102] W. Vansaarloos, Front propagation into unstable states - marginal stability as a dynamical mechanism for velocity selection, Phys. Rev. A 37 (1) (1988) 211–229.
[103] P. Huerre, P.A. Monkewitz, Local and global instabilities in spatially developing flows, Annu. Rev. Fluid Mech. 22 (1990) 473–537.
[104] J.M. Chomaz, Global instabilities in spatially developing flows: non-normality and nonlinearity, Annu. Rev. Fluid Mech. 37 (2005) 357–392.
[105] P. Guillot, A. Ajdari, J. Goyon, M. Joanicot, A. Colin, Droplets and jets in microfluidic devices, C. R. Chim. 12 (1) (2009) 247–257.
[106] Y. Xia, G.M. Whitesides, Soft lithography, Annu. Rev. Mater. Sci. 28 (1) (1998) 153–184.
[107] D. Fuard, T. Tzvetkova-Chevolleau, S. Decossas, P. Tracqui, P. Schiavone, Optimization of poly-di-methyl-siloxane (PDMS) substrates for studying cellular adhesion and motility, Microelectron. Eng. 85 (5–6) (2008) 1289–1293.
[108] J. Zhou, A.V. Ellis, N.H. Voelcker, Recent developments in PDMS surface modification for microfluidic devices, Electrophoresis 31 (1) (2010) 2–16.
[109] J. Kim, M.K. Chaudhury, M.J. Owen, T. Orbeck, The mechanisms of hydrophobic recovery of polydimethylsiloxane elastomers exposed to partial electrical discharges, J. Colloid Interface Sci. 244 (1) (2001) 200–207.
[110] J. Kim, M.K. Chaudhury, M.J. Owen, Hydrophobic recovery of polydimethylsiloxane elastomer exposed to partial electrical discharge, J. Colloid Interface Sci. 226 (2) (2000) 231–236.
[111] L. Yang, N. Shirahata, G. Saini, F. Zhang, L. Pei, M.C. Asplund, D.G. Kurth, K. Ariga, K. Sautter, T. Nakanishi, Effect of surface free energy on PDMS transfer in microcontact printing and its application to ToF-SIMS to probe surface energies, Langmuir 25 (10) (2009) 5674–5683.
[112] A. Utada, E. Lorenceau, D. Link, P. Kaplan, H. Stone, D. Weitz, Monodisperse double emulsions generated from a microcapillary device, Science 308 (5721) (2005) 537–541.
[113] S.A. Nabavi, G.T. Vladisavljević, S. Gu, E.E. Ekanem, Double emulsion production in glass capillary microfluidic device: parametric investigation of droplet generation behaviour, Chem. Eng. Sci. 130 (2015) 183–196.
[114] S. Ross, P. Becher, The history of the spreading coefficient, J. Colloid Interface Sci. 149 (2) (1992) 575–579.
[115] F.S. Bates, Polymer-polymer phase-behavior, Science 251 (4996) (1991) 898–905.
[116] N. Kuwahara, K. Kubota, Spinodal decomposition in a polymer-solution, Phys. Rev. A 45 (10) (1992) 7385–7394.
[117] A. Zwijnenburg, A.J. Pennings, Longitudinal growth of polymer crystals from flowing solutions II. Polyethylene crystals in Poiseuille flow, Colloid Polym. Sci. 253 (6) (1975) 452–461.
[118] B.G. De Geest, J.P. Urbanski, T. Thorsen, J. Demeester, S.C. De Smedt, Synthesis of monodisperse biodegradable microgels in microfluidic devices, Langmuir 21 (23) (2005) 10275–10279.
[119] C.H. Choi, D.A. Weitz, C.S. Lee, One step formation of controllable complex emulsions: from functional particles to simultaneous encapsulation of hydrophilic and hydrophobic agents into desired position, Adv. Mater. 25 (18) (2013) 2536–2541.
[120] T. Nisisako, T. Torii, T. Takahashi, Y. Takizawa, Synthesis of monodisperse bicolored janus particles with electrical anisotropy using a microfluidic co-flow system, Adv. Mater. 18 (9) (2006) 1152–1156.
[121] S.H. Kim, S.Y. Lee, S.M. Yang, Janus microspheres for a highly flexible and impregnable water-repelling Interface, Angew. Chem. Int. Ed. 49 (14) (2010) 2535–2538.
[122] M.F. Haase, J. Brujic, Tailoring of high-order multiple emulsions by the liquid-liquid phase separation of ternary mixtures, Angew. Chem. Int. Ed. 53 (44) (2014) 11793–11797.
[123] C.H. Choi, H. Lee, A. Abbaspourrad, J.H. Kim, J. Fan, M. Caggioni, C. Wesner, T.T. Zhu, D.A. Weitz, Triple emulsion drops with an ultrathin water layer: high encapsulation efficiency and enhanced cargo retention in microcapsules, Adv. Mater. 28 (17) (2016) 3340–3344.
[124] S.H. Kim, S.J. Jeon, S.M. Yang, Optofluidic encapsulation of crystalline colloidal arrays into spherical membrane, J. Am. Chem. Soc. 130 (18) (2008) 6040–6046.
[125] J.W. Kim, A.S. Utada, A. Fernandez-Nieves, Z.B. Hu, D.A. Weitz, Fabrication of monodisperse gel shells and functional microgels in microfluidic devices, Angew. Chem. Int. Ed. 46 (11) (2007) 1819–1822.
[126] E. Lorenceau, A.S. Utada, D.R. Link, G. Cristobal, M. Joanicot, D.A. Weitz, Generation of polymerosomes from double-emulsions, Langmuir 21 (20) (2005) 9183–9186.
[127] H. Zhang, E. Tumarkin, R. Peerani, Z. Nie, R.M.A. Sullan, G.C. Walker, E. Kumacheva, Microfluidic production of biopolymer microcapsules with controlled morphology, J. Am. Chem. Soc. 128 (37) (2006) 12205–12210.
[128] W. Breguet, R. Gugerli, M. Pernetti, U. von Stockar, I.W. Marison, Formation of microcapsules from polyelectrolyte and covalent interactions, Langmuir 21 (21) (2005) 9764–9772.
[129] W.H. Tan, S. Takeuchi, Monodisperse alginate hydrogel microbeads for cell encapsulation, Adv. Mater. 19 (18) (2007) 2696–2701.
[130] D.B. Seifert, J.A. Phillips, Production of small, monodispersed alginate beads for cell immobilization, Biotechnol. Prog. 13 (5) (1997) 562–568.
[131] W.R. Gombotz, S.F. Wee, Protein release from alginate matrices, Adv. Drug Deliv. Rev. 31 (3) (1998) 267–285.
[132] T. Nisisako, T. Torii, T. Higuchi, Novel microreactors for functional polymer beads, Chem. Eng. J. 101 (1–3) (2004) 23–29.
[133] S. Sugiura, T. Oda, Y. Izumida, Y. Aoyagi, M. Satake, A. Ochiai, N. Ohkohchi, M. Nakajima, Size control of calcium alginate beads containing living cells using micro-nozzle array, Biomaterials 26 (16) (2005) 3327–3331.

[134] K. Liu, H.J. Ding, J. Liu, Y. Chen, X.Z. Zhao, Shape-controlled production of biodegradable calcium alginate gel microparticles using a novel microfluidic device, Langmuir 22 (22) (2006) 9453–9457.
[135] Q. Wang, D. Zhang, H.B. Xu, X.L. Yang, A.Q. Shen, Y.J. Yang, Microfluidic one-step fabrication of radiopaque alginate microgels with in situ synthesized barium sulfate nanoparticles, Lab Chip 12 (22) (2012) 4781–4786.
[136] C.H. Choi, J.H. Jung, Y.W. Rhee, D.P. Kim, S.E. Shim, C.S. Lee, Generation of monodisperse alginate microbeads and in situ encapsulation of cell in microfluidic device, Biomed. Microdevices 9 (6) (2007) 855–862.
[137] Y.N. Xia, B. Gates, Y.D. Yin, Y. Lu, Monodispersed colloidal spheres: old materials with new applications, Adv. Mater. 12 (10) (2000) 693–713.
[138] T. Nisisako, T. Torii, T. Higuchi, Droplet formation in a microchannel network, Lab Chip 2 (1) (2002) 24–26.
[139] S. Xu, Z. Nie, M. Seo, P. Lewis, E. Kumacheva, H.A. Stone, P. Garstecki, D.B. Weibel, I. Gitlin, G.M. Whitesides, Generation of monodisperse particles by using microfluidics: control over size, shape, and composition (vol 44, pg 724, 2005), Angew. Chem. Int. Ed. 44 (25) (2005) (3799-3799).
[140] D. Dendukuri, K. Tsoi, T.A. Hatton, P.S. Doyle, Controlled synthesis of nonspherical microparticles using microfluidics, Langmuir 21 (6) (2005) 2113–2116.
[141] A. Perro, S. Reculusa, E. Bourgeat-Lami, E. Duguet, S. Ravaine, Synthesis of hybrid colloidal particles: from snowman-like to raspberry-like morphologies, Colloids Surf. A Physicochem. Eng. Asp. 284 (2006) 78–83.
[142] S. Mitragotri, J. Lahann, Physical approaches to biomaterial design, Nat. Mater. 8 (1) (2009) 15–23.
[143] A. Perro, S. Reculusa, S. Ravaine, E.B. Bourgeat-Lami, E. Duguet, Design and synthesis of Janus micro- and nanoparticles, J. Mater. Chem. 15 (35–36) (2005) 3745–3760.
[144] A. Walther, A.H.E. Muller, Janus particles, Soft Matter 4 (4) (2008) 663–668.
[145] F. Wurm, A.F.M. Kilbinger, Polymeric Janus particles, Angew. Chem. Int. Ed. 48 (45) (2009) 8412–8421.
[146] S.M. Yang, S.H. Kim, J.M. Lim, G.R. Yi, Synthesis and assembly of structured colloidal particles, J. Mater. Chem. 18 (19) (2008) 2177–2190.
[147] S. Jiang, Q. Chen, M. Tripathy, E. Luijten, K.S. Schweizer, S. Granick, Janus particle synthesis and assembly, Adv. Mater. 22 (10) (2010) 1060–1071.
[148] A.B. Pawar, I. Kretzschmar, Fabrication, assembly, and application of patchy particles, Macromol. Rapid Commun. 31 (2) (2010) 150–168.
[149] D. Dendukuri, P.S. Doyle, The synthesis and assembly of polymeric microparticles using microfluidics, Adv. Mater. 21 (41) (2009) 4071–4086.
[150] M.D. McConnell, M.J. Kraeutler, S. Yang, R.J. Composto, Patchy and multiregion Janus particles with tunable optical properties, Nano Lett. 10 (2) (2010) 603–609.
[151] J.R. Howse, R.A.L. Jones, A.J. Ryan, T. Gough, R. Vafabakhsh, R. Golestanian, Self-motile colloidal particles: from directed propulsion to random walk, Phys. Rev. Lett. 99 (4) (2007) 048102–048105.
[152] A. Walther, M. Hoffmann, A.H.E. Muller, Emulsion polymerization using Janus particles as stabilizers, Angew. Chem. Int. Ed. 47 (4) (2008) 711–714.
[153] S.C. Glotzer, M.J. Solomon, Anisotropy of building blocks and their assembly into complex structures, Nat. Mater. 6 (8) (2007) 557–562.
[154] N. Prasad, J. Perumal, C.H. Choi, C.S. Lee, D.P. Kim, Generation of monodisperse inorganic-organic Janus microspheres in a microfluidic device, Adv. Funct. Mater. 19 (10) (2009) 1656–1662.
[155] S.S. Liu, C.F. Wang, X.Q. Wang, J. Zhang, Y. Tian, S.N. Yin, S. Chen, Tunable Janus colloidal photonic crystal supraballs with dual photonic band gaps, J. Mater. Chem. C 2 (44) (2014) 9431–9438.
[156] S. Seiffert, D.A. Weitz, Microfluidic fabrication of smart microgels from macromolecular precursors, Polymer 51 (25) (2010) 5883–5889.
[157] Z.H. Nie, W. Li, M. Seo, S.Q. Xu, E. Kumacheva, Janus and ternary particles generated by microfluidic synthesis: design, synthesis, and self-assembly, J. Am. Chem. Soc. 128 (29) (2006) 9408–9412.
[158] R.F. Shepherd, J.C. Conrad, S.K. Rhodes, D.R. Link, M. Marquez, D.A. Weitz, J.A. Lewis, Microfluidic assembly of homogeneous and Janus colloid-filled hydrogel granules, Langmuir 22 (21) (2006) 8618–8622.
[159] S. Okushima, T. Nisisako, T. Torii, T. Higuchi, Controlled production of monodisperse double emulsions by two-step droplet breakup in microfluidic devices, Langmuir 20 (23) (2004) 9905–9908.
[160] T. Nisisako, S. Okushima, T. Torii, Controlled formulation of monodisperse double emulsions in a multiple-phase microfluidic system, Soft Matter 1 (1) (2005) 23–27.
[161] J.P. Nolan, L.A. Sklar, Suspension array technology: evolution of the flat-array paradigm, Trends Biotechnol. 20 (1) (2002) 9–12.
[162] B. Zheng, J.D. Tice, L.S. Roach, R.F. Ismagilov, A droplet-based, composite PDMS/glass capillary microfluidic system for evaluating protein crystallization conditions by microbatch and vapor-diffusion methods with on-chip X-ray diffraction, Angew. Chem. Int. Ed. 43 (19) (2004) 2508–2511.
[163] B. Zheng, J.D. Tice, R.F. Ismagilov, Formation of droplets of in microfluidic channels alternating composition and applications to indexing of concentrations in droplet-based assays, Anal. Chem. 76 (17) (2004) 4977–4982.
[164] D.K. Hwang, D. Dendukuri, P.S. Doyle, Microfluidic-based synthesis of non-spherical magnetic hydrogel microparticles, Lab Chip 8 (10) (2008) 1640–1647.
[165] C.J.D. Ross, L. Bastedo, S.A. Maier, M.S. Sands, P.L. Chang, Treatment of a lysosomal storage disease, mucopolysaccharidosis VII, with microencapsulated recombinant cells, Hum. Gene Ther. 11 (15) (2000) 2117–2127.
[166] Z.C. Liu, T.M.S. Chang, Transdifferentiation of bioencapsulated bone marrow cells into hepatocyte-like cells in the 90% hepatectomized rat model, Liver Transpl. 12 (4) (2006) 566–572.
[167] P. Cirone, J.M. Bourgeois, P.L. Chang, Antiangiogenic cancer therapy with microencapsulated cells, Hum. Gene Ther. 14 (11) (2003) 1065–1077.
[168] D. Chicheportiche, G. Reach, In vitro kinetics of insulin release by microencapsulated rat islets: effect of the size of the microcapsules, Diabetologia 31 (1) (1988) 54–57.
[169] J.F. Edd, D. Di Carlo, K.J. Humphry, S. Koster, D. Irimia, D.A. Weitz, M. Toner, Controlled encapsulation of single-cells into monodisperse picolitre drops, Lab Chip 8 (8) (2008) 1262–1264.
[170] A. Dove, Cell-based therapies go live, Nat. Biotechnol. 20 (4) (2002) 339–343.
[171] S.A. DeLong, J.J. Moon, J.L. West, Covalently immobilized gradients of bFGF on hydrogel scaffolds for directed cell migration, Biomaterials 26 (16) (2005) 3227–3234.
[172] L.Y. Chu, A.S. Utada, R.K. Shah, J.W. Kim, D.A. Weitz, Controllable monodisperse multiple emulsions, Angew. Chem. Int. Ed. 46 (47) (2007) 8970–8974.
[173] S.H. Kim, D.A. Weitz, One-step emulsification of multiple concentric shells with capillary microfluidic devices, Angew. Chem. Int. Ed. 50 (37) (2011) 8731–8734.
[174] A. Herrmann, Controlled release of volatiles under mild reaction conditions: from nature to everyday products, Angew. Chem. Int. Ed. 46 (31) (2007) 5836–5863.
[175] T. Tree-Udom, S.P. Wanichwecharungruang, J. Seemork, S. Arayachukeat, Fragrant chitosan nanospheres: controlled release systems with physical and chemical barriers, Carbohydr. Polym. 86 (4) (2011) 1602–1609.
[176] A. Sansukcharearnpon, S. Wanichwecharungruang, N. Leepipatpaiboon, T. Kerdcharoen, S. Arayachukeat, High loading fragrance encapsulation based on a polymer-blend: preparation and release behavior, Int. J. Pharm. 391 (1–2) (2010) 267–273.
[177] S. Theisinger, K. Schoeller, B. Osborn, M. Sarkar, K. Landfester, Encapsulation of a fragrance via miniemulsion polymerization for temperature-controlled release, Macromol. Chem. Phys. 210 (6) (2009) 411–420.
[178] A.V. Sadovoy, M.V. Lomova, M.N. Antipina, N.A. Braun, G.B. Sukhorukov, M.V. Kiryukhin, Layer-by-layer assembled multilayer shells for encapsulation and release of fragrance, ACS Appl. Mater. Interfaces 5 (18) (2013) 8948–8954.
[179] H. Lee, C.H. Choi, A. Abbaspourrad, C. Wesner, M. Caggioni, T. Zhu, D.A. Weitz, Encapsulation and enhanced retention of fragrance in polymer microcapsules, ACS Appl. Mater. Interfaces 8 (6) (2016) 4007–4013.